Adipocyte PI3K links adipostasis with insulin secretion through an adipoincretin effect

Barbara Becattini[1], Angela Molinaro[1,2], Marcus Henricsson[1], Jan Borén[1], and Giovanni Solinas[1*]

1 Department of Molecular and Clinical Medicine, Institute of Medicine, University of Gothenburg, Gothenburg, Sweden.

2 Present address: Department of Laboratory Medicine, Institute of Medicine, University of Gothenburg, Gothenburg, Sweden.

[*]Correspondence: giovanni.solinas@wlab.gu.se

Summary

Inhibitors of insulin-PI3K signaling potently induce insulin secretion in-vivo, demonstrating that insulin secretion is governed by feedback control. Resolving the mechanism of this feedback is necessary to understand hyperinsulinemia and insulin resistance and to develop optimal PI3K-targeted therapies. Adipose tissue-specific knockout mice for the insulin receptor, or AKT1 and AKT2, are severely lipodystrophic. Thereby, the role of adipocyte insulin signaling in the feedback control of insulin secretion remains unknown. To investigate insulin-PI3K signaling in the adipocyte in vivo, we generated adipocyte-specific PI3Kα knockout mice (PI3Kα^{AdQ}). PI3Kα^{AdQ} mice and PI3K$\alpha^{F/F}$ control mice showed similar adiposity, indicating compensation from another PI3K activity. PI3Kβ-selective inhibitors dumped AKT phosphorylation, specifically in the adipocytes of PI3Kα^{AdQ} mice. The PI3Kβ-selective inhibitor GSK2636771 markedly increased serum FFA and insulin secretion in PI3Kα^{AdQ} mice but not in PI3K$\alpha^{F/F}$ mice, demonstrating that insulin secretion is governed by adipocyte PI3K, a phenomenon that we name the adipoincretin effect. The adipoincretin effect can be induced in mice fasted overnight with decreasing glycemia. The effects of adipocyte-specific PI3K inhibition on insulin secretion and serum FFA could be partly dissociated by cotreating PI3Kα^{AdQ} mice with GSK2636771 and the lipolysis inhibitor nicotinic acid. The adipoincretin effect was associated with reduced plasma branched-chain amino acids, reduced serum leptin, and increased 3-hydroxybutyrylcarnitine. These results demonstrate that baseline insulin secretion and lipolysis are coregulated by adipocyte PI3K signaling to control adipostasis during fasting through an adipoincretin effect.

Introduction

The current paradigm for the insulin system can be regarded as glucose-centric, with blood glucose being the primary driver of insulin secretion. However, this glucose-centric perspective on the insulin system has been questioned by studies proposing that obesity-associated hyperinsulinemia could be the cause of insulin resistance rather than a mechanism compensating for increased blood glucose (Corkey, 2012; Czech, 2017; Fryk et al., 2021; McGarry, 1992; van Vliet et al., 2020).

Healthy humans with similar glycemia display a large variability in plasma insulin, indicating that the metabolic action of insulin depends on a crosstalk between insulin signaling and insulin secretion (Kahn et al., 1993; Kodama et al., 2013). Substantial variability of insulin secretion is also observed in different mouse strains (Aston-Mourney et al., 2007), and pharmacological inhibition of the insulin receptor (InsR), PI3K, or AKT causes hyperglycemia and hyperinsulinemia in humans and rodents (Ando et al., 2014; Hopkins et al., 2018; Kalinsky et al.,

2018; Patnaik et al., 2016; von Mehren et al., 2020). Thus, insulin secretion is governed by a powerful negative feedback loop induced by InsR-PI3K signaling, which is believed to be driven by insulin action on blood glucose.

PI3K inhibitors cause a potent and sustained induction of insulin secretion in C57BL/6 mice (Hopkins et al., 2018). However, C57BL/6 mice show only a modest and transient increase in plasma insulin in response to an intraperitoneal injection of glucose (Aston-Mourney et al., 2007; Fergusson et al., 2014; Small et al., 2022). Furthermore, hepatocyte-restricted acute inhibition of PI3K activity, achieved by administering a PI3Kβ-selective inhibitor to mice lacking PI3Kα in hepatocytes, causes hyperglycemia without increasing insulin secretion (Molinaro et al., 2019). Altogether, this evidence made us question the current glucose-centric paradigm for the insulin system.

In obese humans with normal glucose tolerance, plasma insulin is higher in subjects with elevated circulating free fatty acids (FFA) and adipose tissue lipolysis (Fryk et al., 2021; Gastaldelli et al., 2017; Kim et al., 2019; van Vliet et al., 2020). In humans and rodents, induction of lipolysis with β-adrenergic agonists stimulates insulin secretion (Imura et al., 1971; Porte, 1967; Sennitt et al., 1985), and inhibition of lipolysis with nicotinic acid (NA) reduces insulin secretion in fasting (Balasse and Ooms, 1973; Boden et al., 1998; Dobbins et al., 1998a; Dobbins et al., 1998b; Stein et al., 1996). Considering the opposing actions of β-adrenergic signaling and InsR-PI3K signaling on adipocyte lipolysis (Guilherme et al., 2022; Solinas and Becattini, 2022), we hypothesized that insulin secretion is governed by adipocyte InsR-PI3K signaling.

Mice lacking either the InsR or AKT1 and AKT2 in their adipocytes develop a severe lipodystrophic phenotype, hepatosteatosis, hyperglycemia, and hyperinsulinemia, demonstrating the requirement for functional insulin signaling in adipostasis (Boucher et al., 2016; Qiang et al., 2016; Sakaguchi et al., 2017; Shearin et al., 2016). However, because of their atrophic adipose tissue and severe metabolic syndrome phenotype, these models provide limited insights into the role of InsR-PI3K signaling within the mature adipocyte in the feedback loop controlling insulin secretion. The mechanisms for the InsR-PI3K feedback control in insulin secretion and the role of the adipocyte in this process remain unknown.

Results

Adipocyte PI3K-AKT signaling depends on PI3Kα and PI3Kβ

It has been proposed that PI3Kα is the main PI3K catalytic isoform in adipocyte insulin signaling (Foukas et al., 2006; Knight et al., 2006). Therefore, we crossed PI3Kα LoxP floxed mice

(PI3K$\alpha^{F/F}$) (Molinaro et al., 2019) with mice expressing the Cre recombinase under the control of the AdipoQ promoter to generate mice lacking PI3Kα specifically in adipocytes (PI3Kα^{AdQ}). Compared to PI3K$\alpha^{F/F}$ mice, PI3Kα^{AdQ} mice showed a substantial reduction of PI3Kα protein abundance in fat pads but not in other tissues (Figure S1A-D). Mature adipocytes purified from epididymal fat pads of PI3Kα^{AdQ} mice showed almost complete ablation of the PI3Kα protein without changes in the abundance of the other PI3K subunits or IRS1 and IRS2 (Figure S1E and F). PI3Kα protein abundance was not affected in adipose tissue stromal vascular cells of PI3Kα^{AdQ} mice (Figure S1G and H).

PI3Kα^{AdQ} mice showed a normal growth curve, slightly reduced serum FFA levels, normal fasting glucose and insulin levels, normal glucose and insulin tolerance, and normal suppression of serum FFA levels by glucose (Figures 1A-C and S2A-C). Fat pad weights and adipocyte size distribution of PI3Kα^{AdQ} mice were similar to controls, and their liver histology was normal (Figures 1D-F and S2D). We conclude that, unlike mice with InsR or AKT1 and AKT2 ablation in their adipocytes, PI3Kα^{AdQ} mice are not lipodystrophic and show normal glucose and lipid homeostasis. Therefore, another PI3K activity compensates for the absence of PI3Kα in adipocyte insulin signaling.

To identify the PI3K isoforms driving AKT phosphorylation in the adipocyte, PI3K$\alpha^{F/F}$ mice and PI3Kα^{AdQ} mice were fasted for 12 hours and received an intraperitoneal injection (i.p.) of 2 g/kg of glucose in the presence of different isoform-selective PI3K inhibitors or vehicle. Ten minutes after the injection, the mice were sacrificed, and the epididymal fat pads were collected to measure AKT phosphorylation. AKT phosphorylation was similar in the adipose tissues of PI3K$\alpha^{F/F}$ mice and PI3Kα^{AdQ} mice injected with glucose and vehicle (Figure 1G). The PI3Kγ-selective inhibitor IPI549 or the PI3Kδ-selective inhibitor PIK294 did not affect AKT phosphorylation in the adipose tissues of PI3Kα^{AdQ} mice. However, two different PI3Kβ-selective inhibitors (TGX221 and GSK2636771) substantially reduced AKT phosphorylation in the adipose tissue of PI3Kα^{AdQ} mice, with GSK2636771 achieving more than 90% inhibition (Figure 1G). In PI3K$\alpha^{F/F}$ control mice, TGX221 and GSK2636771 had no significant effect on adipose tissue AKT phosphorylation (Figure 1H).

These results demonstrate that mouse adipocyte PI3K-AKT signaling in vivo depends on redundant PI3Kα and PI3Kβ activities.

Adipocyte PI3K links adipostasis with insulin secretion

The results described above indicate that PI3K signaling can be inhibited selectively in the adipocytes of PI3Kα^{AdQ} mice in vivo by administering a PI3Kβ-specific inhibitor (Figure 1G). We named this approach "catalytic activity of PI3K inhibited in selected cells (CAPISCe)", and we used it to investigate the role of adipose tissue PI3K signaling in the feedback loop governing insulin secretion.

PI3K$\alpha^{F/F}$ mice and PI3Kα^{AdQ} mice were fasted for 12 hours and received an intraperitoneal injection of 2 g/kg of glucose with either vehicle or the PI3Kβ-selective inhibitor GSK2636771. Blood glucose levels were similar between groups, and serum FFA levels were significantly reduced following the glucose injection in all the groups except for the PI3Kα^{AdQ} mice treated with GSK2636771, where serum FFA abundance was substantially increased (Figure 2A and B). Serum insulin and C-peptide (a marker for insulin secretion) were close to basal levels in all groups except for PI3Kα^{AdQ} mice treated with GSK2636771, where insulin secretion within 30 minutes was potently induced in a sustained manner (Figure 2C and D). These results reveal that adipocyte PI3K activity suppresses a feedback signal driving insulin secretion. By analogy to the glucoincretin effect (Holst, 2019; Rehfeld, 2018), we named this phenomenon "the adipoincretin effect." A similar, although less potent, effect was observed in PI3Kα^{AdQ} mice treated with TGX221 (Figure S3). TGX221, which was less effective than GSK2636771 in reducing AKT phosphorylation in adipocytes (Figure 1G), blocked the action of glucose on FFA suppression but did not increase FFA above basal levels (Figure S3B). Hence, the adipoincretin effect can be in part dissociated from increased serum FFA. TGX221 and GSK2636771 had no effect on insulin secretion in cultured islets from PI3K$\alpha^{F/F}$ mice or PI3Kα^{AdQ} mice, which excludes a direct action of PI3Kβ-specific inhibition on the islets (Figure S3D).

A cohort of mice was sacrificed one hour after the GSK2636771 injection, and AKT phosphorylation was measured in different tissues. GSK2636771 showed no effect on AKT or ERK phosphorylation in PI3K$\alpha^{F/F}$ mice but substantially reduced AKT phosphorylation, without affecting ERK phosphorylation, in the adipose tissues of PI3Kα^{AdQ} mice (Figures 2E, F, and Figure S4). We observed increased AKT Ser-473 phosphorylation in the liver and muscle of PI3Kα^{AdQ} mice treated with GSK2636771 (Figure 2E, F), which is coherent with an adipose-specific PI3K inhibition and the increased insulin levels observed in these mice.

We conclude that adipocyte PI3K signaling links insulin secretion with adipostasis through the adipoincretin effect.

The adipoincretin effect operates independently from glucose administration and the feeding state

The adipoincretin effect was vastly more potent than the effect on insulin secretion caused by an intraperitoneal injection of 2 g/kg of glucose (Figure 2A and C, D). Therefore, we investigated the dependency of the adipoincretin effect on glucose administration and feeding state.

Injection of GSK2636771, without glucose, significantly increased serum FFA and induced insulin secretion specifically in PI3Kα^{AdQ} mice but not in littermate control PI3K$\alpha^{F/F}$ mice, in either fed conditions (Figure 3A-D) or after overnight fasting (Figure 3E-G).

In PI3Kα^{AdQ} mice starved overnight, serum insulin kept increasing after GSK2636771 injection despite blood glucose being reduced (Figure 3E-G), with one mouse showing 0.43 ng/ml of insulin and 6.1 mmol/l of glucose before injection and 4.3 ng/ml of insulin and 2.5 mmol/l of glucose 180 minutes post-injection. Thus, the adiposecretin effect is not driven by increased blood glucose and can operate in hypoglycemic mice. The mice showed no sign of a hypoglycemic crisis during the experiment, most likely because of increased lipolysis.

Leptin is an insulin-regulated adipokine (Saladin et al., 1995), that controls adipostasis and insulin secretion (Coleman and Hummel, 1974; Covey et al., 2006). Therefore, we measured serum leptin levels in PI3K$\alpha^{F/F}$ and PI3Kα^{AdQ} fasted mice after GSK2636771 injection. Compared to PI3K$\alpha^{F/F}$ mice, PI3Kα^{AdQ} mice showed reduced leptin levels (Figure 3H). However, this difference in serum leptin was significant only 180 minutes after the GSK2636771 injection.

We conclude that the adipoincretin effect does not require increased blood glucose, operates in fed and fasting conditions over a broad range of blood glucose concentrations, and is not initiated by a reduction of serum leptin.

Contribution of lipolysis to the adipoincretin effect

FFA promote insulin secretion in cultured islets by binding to the GPR40 receptor on β-cells (Itoh et al., 2003). In vivo, β-adrenergic agonists induce lipolysis and stimulate insulin secretion (Imura et al., 1971; Porte, 1967; Sennitt et al., 1985). Furthermore, inhibition of lipolysis with nicotinic acid (NA) was reported to reduce insulin secretion in fasting (Balasse and Ooms, 1973; Boden et al., 1998; Dobbins et al., 1998a; Dobbins et al., 1998b; Stein et al., 1996). Therefore, we have investigated the contribution of lipolysis and increased FFA to the insulin secretion induced by systemic PI3K inhibition.

Wild-type (WT) C57Bl6/J mice were fasted overnight and injected intraperitoneally with either Buparlisib (8 mg/kg) or Taselisib (3.5 mg/kg), two different pan-PI3K inhibitors, in the presence or absence of NA (100 mg/kg). NA did not affect the blood glucose levels of mice treated with

Buparlisib but dumped serum FFA (Figure 4A and B). As expected, 8 mg of Buparlisib significantly increased insulin secretion (Figure 4C). However, this effect was less potent than the one we typically observed in PI3Kα^{AdQ} mice treated with 6 mg/kg of GSK2636771, indicating a partial PI3K inhibition. Compared to mice treated with Buparlisib alone, mice cotreated with Buparlisib and NA showed a trend toward a reduced increase of serum insulin (Figure 4C). However, despite a substantial reduction of serum FFA, the effect of NA on serum insulin was partial and did not achieve statistical significance.

WT mice injected with 3.5 mg/kg of Taselisib showed increased blood glucose, serum FFA, and substantially elevated serum insulin (Figure 4D-F). Cotreatment with NA dumped serum FFA, and although Taselisib increased serum insulin also in the presence of NA, NA significantly reduced the increase of serum insulin induced by Taselisib (Figure 4D-F). This finding was reproduced in an independent cohort of mice in fasting and fed conditions (Figure S5A-F). Hence, the effects of systemic PI3K inhibition on insulin secretion can be reduced by inhibiting lipolysis with NA.

We have investigated the contribution of lipolysis to the adipoincretin effect. PI3Kα^{AdQ} mice were fasted overnight and injected with 6 mg/kg of GSK2636771 alone or 6 mg/kg of GSK2636771 with 100 mg/kg NA. Blood glucose levels were similar between groups and decreased during the experiment (Figure 4G). Serum FFA abundance was increased over the baseline by GSK2636771 and dumped by the NA cotreatment (Figure 4H). GSK2636771 increased serum insulin levels in PI3Kα^{AdQ} mice cotreated with NA (Figure 4I). We observed a substantial trend toward a reduced adipoincretin effect in PI3Kα^{AdQ} mice treated with GSK2636771 in the presence of NA. However, this reduction was not statistically significant (Figure 4I). This finding was reproduced in an independent cohort (Figure S5G-I).

To summarize, for any PI3K inhibitor and condition tested, we have always observed that NA partially reduced serum insulin; this reduction was statistically significant for WT mice treated with Taselisib and was not associated with a reduction in blood glucose level.

We conclude that the adipoincretin effect and the effects of systemic PI3K inhibition on insulin secretion are partially dependent on increased lipolysis and that another PI3K-regulated but FFA-independent signal from the adipocyte contributes to the adipoincretin effect.

The adipoincretin effect is associated with reduced plasma BCAA and increased 3OH-4C-carnitine

We have investigated the role of candidate adipokines and metabolites in the adipoincretin effect. PI3K$\alpha^{F/F}$ mice and PI3Kα^{AdQ} mice were fasted overnight and sacrificed at 30 or 90

minutes after the GSK2636771 injection. Adipose tissues and plasma from the mice above were collected before the GSK2636771 injection and at sacrifice. Compared to baseline levels, the plasma abundance of C-peptide was substantially increased 30 and 90 minutes after GSK2636771 injection in PI3Kα^{AdQ} mice but not in PI3K$\alpha^{F/F}$ control mice (Figures 5A and S6A). Blood glucose levels were similar in PI3K$\alpha^{F/F}$ and PI3Kα^{AdQ} mice 30 minutes after GSK2636771 injection and slightly reduced in PI3Kα^{AdQ} mice 90 minutes after GSK2636771 (Figures 5B and S6B). Plasma abundances of adipsin and FABP4, two adipokines that have been implicated in basal insulin secretion (Lo et al., 2014) and lipolysis-associated insulin secretion (Scheja et al., 1999) respectively, were similar in PI3K$\alpha^{F/F}$ and PI3Kα^{AdQ} mice at 30 and 90 minutes after GSK2636771 (Figure S7).

The branched-chain amino acid (BCAA) leucine, in combination with glutamine, potently induces insulin secretion in cultured β-cells (Sener and Malaisse, 1980). PI3K$\alpha^{F/F}$ and PI3Kα^{AdQ} mice showed similar plasma glutamine levels at all time points, but plasma BCAA abundances were significantly reduced in PI3Kα^{AdQ} mice compared to PI3K$\alpha^{F/F}$ control mice 90' after GSK2636771 (Figures 5C, D and S5C, D). Branched-chain ketoacids (BCKA) plasma levels were virtually identical in PI3K$\alpha^{F/F}$ and PI3Kα^{AdQ} mice (Figures 5E and S5E).

To further learn about the effects of adipocyte PI3K inhibition on fatty acids metabolism, we measured the abundance of acyl-carnitines in the plasma of the mice above. Compared to control PI3K$\alpha^{F/F}$ mice, PI3Kα^{AdQ} mice showed an increased abundance of plasma 3-hydroxybutyrylcarnitine (3OH-4C-Carnitine) 90' after the GSK2636771 injection (Figure 5F). Other acylcarnitines and free carnitine were not altered (Figures 5F and S5F).

These results indicate that the adipoincretin effect is not associated with increased plasma adipsin, FABP4, glutamine, or BCKA but was associated with reduced BCAA and increased 3OH-4C-Carnitine.

Discussion

The induction of insulin secretion by food and glucose is relatively well understood (Campbell and Newgard, 2021; Rorsman and Ashcroft, 2018), but the mechanisms controlling basal insulin secretion during fasting and the interorgan crosstalk between insulin action and insulin secretion remain unresolved. We now report that basal insulin secretion by the pancreatic β-cell and adipocyte lipolysis are coregulated by redundant PI3Kα and PI3Kβ activities within the adipocyte through the adipoincretin effect.

Acute adipocyte-selective PI3K inhibition blocked the effect of glucose on lipolysis and increased serum FFA in mice fasted overnight, demonstrating the potent action of adipocyte PI3K signaling in the control of lipolysis and adipostasis during starvation. This finding extends previous studies showing that mice with adipocyte-specific deletion of the insulin receptor or AKT1 and AKT2, develop severe lipodystrophy (Boucher et al., 2016; Sakaguchi et al., 2017; Shearin et al., 2016). Indeed, our results show that the action of insulin-PI3K signaling in adipostasis is not limited to the fed condition but controls the rate of lipolysis also during prolonged fasting.

Most importantly, we discovered that acute inhibition of adipocyte PI3K activity causes a substantial and sustained increase in insulin secretion, revealing that adipocyte PI3K signaling controls a feedback loop inhibiting insulin secretion. This phenomenon, which we named the adipoincretin effect, is induced by acute inhibition of adipocyte PI3K activity independently from the feeding state. However, because the adipoincretin effect is triggered by low adipocyte PI3K activity in association with elevated lipolysis, it is logical to deduce that the physiological function of the adipoincretin effect is to control the rate of lipolysis during fasting.

Thus, whereas the insulin secretion response to food is governed by the feedforward control from the glucoincretin effect, cephalic phase, and increased blood glucose (Berthoud et al., 1981; Nauck et al., 1986), basal insulin secretion during fasting depends on the feedback control from adipocyte PI3K activity through the adipoincretin effect (Figure 6). This concept stands in stark contrast to the glucose-focused paradigm of the insulin system and implicates that the insulin system is an adipostat, with insulin-PI3K signaling in the adipocyte acting as a “cruise control” for lipolysis during fasting through the adipoincretin feedback loop. Combining the glucoincretin feedforward control of the feeding response with the adipoincretin feedback loop during fasting (Figure 6) has the advantage of separating the control of food-induced insulin secretion from the control of baseline insulin secretion during starvation, optimizing the two processes (Åström and Murray, 2008).

It was reported that adipocyte insulin signaling controls hepatic glucose production during fasting when liver glycogen is depleted (Perry et al., 2015; Petersen and Shulman, 2018; Titchenell et al., 2017; Titchenell et al., 2016). However, the adipoincretin effect was also induced in the fed condition and was not associated with increased blood glucose, and in fasted mice, it occurred while blood glucose was decreasing from more than six mmo/l to about three mmol/l (Figure 3E and G). Finally, the effect of adipocyte PI3K inhibition on insulin secretion was far more potent than that caused by an intraperitoneal injection of 2 g/kg of glucose. Hence, the adipoincretin effect cannot be explained by lipolysis driving endogenous glucose production.

Activation of lipolysis by β-adrenergic agonists is known to induce insulin secretion independently from blood glucose (Grujic et al., 1997; Imura et al., 1971; Porte, 1967; Yoshida, 1992). However, we could partially dissociate the adipoincretin effect from increased FFA by co-treating PI3Kα^{AdQ} mice with the PI3Kβ-selective inhibitor GSK2636771 in the presence of NA or by using the less potent PI3Kβ-selective inhibitor TGX221.

We have also found that the adipoincretin effect is associated with reduced plasma abundance of BCAA, showing that the adipoincretin effect is not driven by leucine and that the adipoincretin effect controls fasting plasma abundances of BCAA.

The glucoincretin effect may be mediated by specific adipokines. A logical candidate is leptin, a crucial adipostatic signal whose circulating levels are induced by insulin and feeding (Ahima et al., 1996; Saladin et al., 1995; Trayhurn et al., 1995). Mice lacking functional leptin signaling develop hyperinsulinemia and mild hypoglycemia before becoming obese (Coleman and Hummel, 1974; Covey et al., 2006), and correcting the insulin levels prevents obesity in leptin-deficient mice (D'Souza A et al., 2016). Compared to control mice, mice with adipocyte-selective PI3K inhibition showed reduced serum leptin, but this difference was significant only by the end of the experiment, after the induction of insulin secretion. We conclude that the adipoincretin effect is not initiated by the reduced abundance of circulating leptin. However, we believe that low circulating leptin abundance drives insulin secretion after a prolonged period of starvation when the adipose tissue is progressively depleted. This view is supported by a study showing that inducible ablation of the insulin receptor in adipocytes of adult mice within a few days causes severe lipoatrophy and hypoleptinemia in association with hyperinsulinemia that can be corrected by continuous leptin infusion (Sakaguchi et al., 2017).

Another candidate “adipo-incretin” is adipsin, also known as complement factor D, as mice lacking adipsin display reduced fasting insulin (Lo et al., 2014). Adipocyte-specific PI3K inhibition did not affect plasma adipsin abundance. However, our results do not exclude a possible function of adipocyte PI3K in controlling adipsin activity on insulin secretion.

A third candidate adipo-incretin is FABP4, which has been implicated in the induction of insulin secretion by β-adrenergic agonists, which also induce lipolysis (Scheja et al., 1999). We have found that adipocyte-specific PI3K inhibition has no effect on the circulating levels of FABP4, and a recent study indicates that lipolysis-associated insulin secretion is largely independent of FABP4 expression in the adipocyte but depends on FABP4 in endothelial cells (Inouye et al., 2022). It is thus unlikely that the adipoincretin effect is driven by PI3K action on FABP4 within the adipocyte. However, adipocyte PI3K signaling may inhibit the release of a factor controlling systemic FABP4 activity on insulin secretion.

We have found that the plasma abundance of 3OH-4C-Carnitine was significantly elevated in mice 90 minutes after adipocyte-selective PI3K inhibition. 3OH-4C-Carnitine is elevated in humans affected by a form of hyperinsulinism caused by loss of function mutations on the gene encoding for L-3-hydroxyacyl-CoA-dehydrogenase (HADH) (Clayton et al., 2001). However, the role of adipocyte HADH activity in insulin secretion remains unresolved, and more research is needed to understand the significance of increased 3OH-4C-Carnitine on insulin secretion.
The precise nature of the adipocyte-derived feedback signal mediating the adipoincretin effect remains unresolved, and future research is granted. Nevertheless, the discovery of the adipoincretin effect transforms our understanding of the insulin system and adipostasis with an impact on the research fields of obesity, diabetes, and cancer.
The hyperinsulinemia induced by inhibition of PI3K signaling was shown to dampen the efficacy of PI3K-targeted cancer therapy (Hopkins et al., 2018). Cell-permeable hydrophobic molecules, such as the PI3K inhibitors, typically accumulate in the adipose tissue, and our study shows that inhibition of adipocyte PI3K activity induces insulin secretion independently from blood glucose through the adipoincretin effect. We have found that NA significantly reduced the hyperinsulinemia induced by the pan PI3K inhibitor Taselisib. Future research will test whether NA supplementation improves the efficacy of PI3K inhibitors in cancer therapies.
It was proposed that in obese subjects with normal glucose tolerance, hyperinsulinemia can be explained mainly by increased baseline insulin secretion at fasting (Polonsky et al., 1988). Because adipose tissue lipolysis and fasting serum insulin are associated in obese subjects (Fryk et al., 2021), the development of hyperinsulinemia and insulin resistance in obesity may be driven by an exacerbated adipoincretin effect due to increased fat mass.
Future research on the adipoincretin effect holds great promise for the development of targeted therapies for cancer, obesity, and type-2 diabetes.

ACKNOWLEDGMENTS: We are grateful to Prof. Claes Wollheim at Lund University for our conversations on β-cell biology and to Prof. Paolo De Los Rios at the EPFL for our conversations on the properties of feedback control systems.

FUNDING: This study is supported by grants from the Novo Nordisk Foundation, the Swedish Research Council, the Cancerfonden, and the Diabetesfonden to G.S.

CONTRIBUTIONS: B.B codesigned and performed most experiments, interpreted data, and contributed to writing the manuscript; A.M generated the PI3Kα^{AdQ} mice and characterized the

PI3Kα deletion; M.H. and J.B. performed targeted metabolomics; all authors have read and approved the manuscript; G.S. conceived the study, analyzed, and interpreted the results, and wrote the first version of the manuscript.

REFERENCES

Ahima, R.S., Prabakaran, D., Mantzoros, C., Qu, D., Lowell, B., Maratos-Flier, E., and Flier, J.S. (1996). Role of leptin in the neuroendocrine response to fasting. Nature *382*, 250-252.

Ando, Y., Inada-Inoue, M., Mitsuma, A., Yoshino, T., Ohtsu, A., Suenaga, N., Sato, M., Kakizume, T., Robson, M., Quadt, C.*, et al.* (2014). Phase I dose-escalation study of buparlisib (BKM120), an oral pan-class I PI3K inhibitor, in Japanese patients with advanced solid tumors. Cancer Sci *105*, 347-353.

Aston-Mourney, K., Wong, N., Kebede, M., Zraika, S., Balmer, L., McMahon, J.M., Fam, B.C., Favaloro, J., Proietto, J., Morahan, G.*, et al.* (2007). Increased nicotinamide nucleotide transhydrogenase levels predispose to insulin hypersecretion in a mouse strain susceptible to diabetes. Diabetologia *50*, 2476-2485.

Åström, K.J., and Murray, R.M. (2008). Feedback Systems: An Introduction for Scientists and Engineers (Princeton University Press).

Balasse, E.O., and Ooms, H.A. (1973). Role of plasma free fatty acids in the control of insulin secretion in man. Diabetologia *9*, 145-151.

Berthoud, H.R., Bereiter, D.A., Trimble, E.R., Siegel, E.G., and Jeanrenaud, B. (1981). Cephalic phase, reflex insulin secretion. Neuroanatomical and physiological characterization. Diabetologia *20 Suppl*, 393-401.

Boden, G., Chen, X., and Iqbal, N. (1998). Acute lowering of plasma fatty acids lowers basal insulin secretion in diabetic and nondiabetic subjects. Diabetes *47*, 1609-1612.

Boucher, J., Softic, S., El Ouaamari, A., Krumpoch, M.T., Kleinridders, A., Kulkarni, R.N., O'Neill, B.T., and Kahn, C.R. (2016). Differential Roles of Insulin and IGF-1 Receptors in Adipose Tissue Development and Function. Diabetes *65*, 2201-2213.

Campbell, J.E., and Newgard, C.B. (2021). Mechanisms controlling pancreatic islet cell function in insulin secretion. Nat Rev Mol Cell Biol *22*, 142-158.

Clayton, P.T., Eaton, S., Aynsley-Green, A., Edginton, M., Hussain, K., Krywawych, S., Datta, V., Malingre, H.E., Berger, R., and van den Berg, I.E. (2001). Hyperinsulinism in short-chain L-3-hydroxyacyl-CoA dehydrogenase deficiency reveals the importance of beta-oxidation in insulin secretion. J Clin Invest *108*, 457-465.

Coleman, D.L., and Hummel, K.P. (1974). Hyperinsulinemia in pre-weaning diabetes (db) mice. Diabetologia *10 Suppl*, 607-610.
Corkey, B.E. (2012). Banting lecture 2011: hyperinsulinemia: cause or consequence? Diabetes *61*, 4-13.
Covey, S.D., Wideman, R.D., McDonald, C., Unniappan, S., Huynh, F., Asadi, A., Speck, M., Webber, T., Chua, S.C., and Kieffer, T.J. (2006). The pancreatic beta cell is a key site for mediating the effects of leptin on glucose homeostasis. Cell Metab *4*, 291-302.
Czech, M.P. (2017). Insulin action and resistance in obesity and type 2 diabetes. Nat Med *23*, 804-814.
D'Souza A, M., Johnson, J.D., Clee, S.M., and Kieffer, T.J. (2016). Suppressing hyperinsulinemia prevents obesity but causes rapid onset of diabetes in leptin-deficient Lep(ob/ob) mice. Mol Metab *5*, 1103-1112.
Dobbins, R.L., Chester, M.W., Daniels, M.B., McGarry, J.D., and Stein, D.T. (1998a). Circulating fatty acids are essential for efficient glucose-stimulated insulin secretion after prolonged fasting in humans. Diabetes *47*, 1613-1618.
Dobbins, R.L., Chester, M.W., Stevenson, B.E., Daniels, M.B., Stein, D.T., and McGarry, J.D. (1998b). A fatty acid- dependent step is critically important for both glucose- and non-glucose-stimulated insulin secretion. J Clin Invest *101*, 2370-2376.
Fergusson, G., Ethier, M., Guevremont, M., Chretien, C., Attane, C., Joly, E., Fioramonti, X., Prentki, M., Poitout, V., and Alquier, T. (2014). Defective insulin secretory response to intravenous glucose in C57Bl/6J compared to C57Bl/6N mice. Mol Metab *3*, 848-854.
Foukas, L.C., Claret, M., Pearce, W., Okkenhaug, K., Meek, S., Peskett, E., Sancho, S., Smith, A.J., Withers, D.J., and Vanhaesebroeck, B. (2006). Critical role for the p110alpha phosphoinositide-3-OH kinase in growth and metabolic regulation. Nature *441*, 366-370.
Fryk, E., Olausson, J., Mossberg, K., Strindberg, L., Schmelz, M., Brogren, H., Gan, L.M., Piazza, S., Provenzani, A., Becattini, B.*, et al.* (2021). Hyperinsulinemia and insulin resistance in the obese may develop as part of a homeostatic response to elevated free fatty acids: A mechanistic case-control and a population-based cohort study. EBioMedicine *65*, 103264.
Gastaldelli, A., Gaggini, M., and DeFronzo, R.A. (2017). Role of Adipose Tissue Insulin Resistance in the Natural History of Type 2 Diabetes: Results From the San Antonio Metabolism Study. Diabetes *66*, 815-822.
Grujic, D., Susulic, V.S., Harper, M.E., Himms-Hagen, J., Cunningham, B.A., Corkey, B.E., and Lowell, B.B. (1997). Beta3-adrenergic receptors on white and brown adipocytes mediate beta3-

selective agonist-induced effects on energy expenditure, insulin secretion, and food intake. A study using transgenic and gene knockout mice. J Biol Chem *272*, 17686-17693.
Guilherme, A., Rowland, L.A., Wang, H., and Czech, M.P. (2022). The adipocyte supersystem of insulin and cAMP signaling. Trends Cell Biol.
Holst, J.J. (2019). From the Incretin Concept and the Discovery of GLP-1 to Today's Diabetes Therapy. Front Endocrinol (Lausanne) *10*, 260.
Hopkins, B.D., Pauli, C., Du, X., Wang, D.G., Li, X., Wu, D., Amadiume, S.C., Goncalves, M.D., Hodakoski, C., Lundquist, M.R.*, et al.* (2018). Suppression of insulin feedback enhances the efficacy of PI3K inhibitors. Nature *560*, 499-503.
Imura, H., Kato, Y., Ikeda, M., Morimoto, M., and Yawata, M. (1971). Effect of adrenergic-blocking or -stimulating agents on plasma growth hormone, immunoreactive insulin, and blood free fatty acid levels in man. J Clin Invest *50*, 1069-1079.
Inouye, K.E., Prentice, K.J., Lee, A., Dominguez-Gonzalez, C., Chen, M.X., Lee, G.Y., and Hotamisligil, G.S. (2022). Endothelial FABP4 constitutes the majority of basal circulating hormone levels and regulates lipolysis-driven insulin secretion. bioRxiv, 2022.2010. 2013.511807.
Itoh, Y., Kawamata, Y., Harada, M., Kobayashi, M., Fujii, R., Fukusumi, S., Ogi, K., Hosoya, M., Tanaka, Y., Uejima, H.*, et al.* (2003). Free fatty acids regulate insulin secretion from pancreatic beta cells through GPR40. Nature *422*, 173-176.
Kahn, S.E., Prigeon, R.L., McCulloch, D.K., Boyko, E.J., Bergman, R.N., Schwartz, M.W., Neifing, J.L., Ward, W.K., Beard, J.C., Palmer, J.P.*, et al.* (1993). Quantification of the relationship between insulin sensitivity and beta-cell function in human subjects. Evidence for a hyperbolic function. Diabetes *42*, 1663-1672.
Kalinsky, K., Sparano, J.A., Zhong, X., Andreopoulou, E., Taback, B., Wiechmann, L., Feldman, S.M., Ananthakrishnan, P., Ahmad, A., Cremers, S.*, et al.* (2018). Pre-surgical trial of the AKT inhibitor MK-2206 in patients with operable invasive breast cancer: a New York Cancer Consortium trial. Clin Transl Oncol *20*, 1474-1483.
Kim, J.Y., Bacha, F., Tfayli, H., Michaliszyn, S.F., Yousuf, S., and Arslanian, S. (2019). Adipose Tissue Insulin Resistance in Youth on the Spectrum From Normal Weight to Obese and From Normal Glucose Tolerance to Impaired Glucose Tolerance to Type 2 Diabetes. Diabetes Care *42*, 265-272.
Knight, Z.A., Gonzalez, B., Feldman, M.E., Zunder, E.R., Goldenberg, D.D., Williams, O., Loewith, R., Stokoe, D., Balla, A., Toth, B.*, et al.* (2006). A pharmacological map of the PI3-K family defines a role for p110alpha in insulin signaling. Cell *125*, 733-747.

Kodama, K., Tojjar, D., Yamada, S., Toda, K., Patel, C.J., and Butte, A.J. (2013). Ethnic differences in the relationship between insulin sensitivity and insulin response: a systematic review and meta-analysis. Diabetes Care *36*, 1789-1796.
Lo, J.C., Ljubicic, S., Leibiger, B., Kern, M., Leibiger, I.B., Moede, T., Kelly, M.E., Chatterjee Bhowmick, D., Murano, I., Cohen, P.*, et al.* (2014). Adipsin is an adipokine that improves beta cell function in diabetes. Cell *158*, 41-53.
McGarry, J.D. (1992). What if Minkowski had been ageusic? An alternative angle on diabetes. Science *258*, 766-770.
Molinaro, A., Becattini, B., Mazzoli, A., Bleve, A., Radici, L., Maxvall, I., Sopasakis, V.R., Molinaro, A., Backhed, F., and Solinas, G. (2019). Insulin-Driven PI3K-AKT Signaling in the Hepatocyte Is Mediated by Redundant PI3Kalpha and PI3Kbeta Activities and Is Promoted by RAS. Cell Metab *29*, 1400-1409 e1405.
Nauck, M.A., Homberger, E., Siegel, E.G., Allen, R.C., Eaton, R.P., Ebert, R., and Creutzfeldt, W. (1986). Incretin effects of increasing glucose loads in man calculated from venous insulin and C-peptide responses. J Clin Endocrinol Metab *63*, 492-498.
Patnaik, A., Appleman, L.J., Tolcher, A.W., Papadopoulos, K.P., Beeram, M., Rasco, D.W., Weiss, G.J., Sachdev, J.C., Chadha, M., Fulk, M.*, et al.* (2016). First-in-human phase I study of copanlisib (BAY 80-6946), an intravenous pan-class I phosphatidylinositol 3-kinase inhibitor, in patients with advanced solid tumors and non-Hodgkin's lymphomas. Ann Oncol *27*, 1928-1940.
Perry, R.J., Camporez, J.G., Kursawe, R., Titchenell, P.M., Zhang, D., Perry, C.J., Jurczak, M.J., Abudukadier, A., Han, M.S., Zhang, X.M.*, et al.* (2015). Hepatic acetyl CoA links adipose tissue inflammation to hepatic insulin resistance and type 2 diabetes. Cell *160*, 745-758.
Petersen, M.C., and Shulman, G.I. (2018). Mechanisms of Insulin Action and Insulin Resistance. Physiol Rev *98*, 2133-2223.
Polonsky, K.S., Given, B.D., and Van Cauter, E. (1988). Twenty-four-hour profiles and pulsatile patterns of insulin secretion in normal and obese subjects. J Clin Invest *81*, 442-448.
Porte, D., Jr. (1967). Beta adrenergic stimulation of insulin release in man. Diabetes *16*, 150-155.
Qiang, G., Whang Kong, H., Xu, S., Pham, H.A., Parlee, S.D., Burr, A.A., Gil, V., Pang, J., Hughes, A., Gu, X.*, et al.* (2016). Lipodystrophy and severe metabolic dysfunction in mice with adipose tissue-specific insulin receptor ablation. Mol Metab *5*, 480-490.
Rehfeld, J.F. (2018). The Origin and Understanding of the Incretin Concept. Front Endocrinol (Lausanne) *9*, 387.

Rorsman, P., and Ashcroft, F.M. (2018). Pancreatic beta-Cell Electrical Activity and Insulin Secretion: Of Mice and Men. Physiol Rev *98*, 117-214.
Sakaguchi, M., Fujisaka, S., Cai, W., Winnay, J.N., Konishi, M., O'Neill, B.T., Li, M., Garcia-Martin, R., Takahashi, H., Hu, J.*, et al.* (2017). Adipocyte Dynamics and Reversible Metabolic Syndrome in Mice with an Inducible Adipocyte-Specific Deletion of the Insulin Receptor. Cell Metab *25*, 448-462.
Saladin, R., De Vos, P., Guerre-Millo, M., Leturque, A., Girard, J., Staels, B., and Auwerx, J. (1995). Transient increase in obese gene expression after food intake or insulin administration. Nature *377*, 527-529.
Scheja, L., Makowski, L., Uysal, K.T., Wiesbrock, S.M., Shimshek, D.R., Meyers, D.S., Morgan, M., Parker, R.A., and Hotamisligil, G.S. (1999). Altered insulin secretion associated with reduced lipolytic efficiency in aP2-/- mice. Diabetes *48*, 1987-1994.
Sener, A., and Malaisse, W.J. (1980). L-leucine and a nonmetabolized analogue activate pancreatic islet glutamate dehydrogenase. Nature *288*, 187-189.
Sennitt, M.V., Arch, J.R., Levy, A.L., Simson, D.L., Smith, S.A., and Cawthorne, M.A. (1985). Anti-hyperglycaemic action of BRL 26830, a novel beta-adrenoceptor agonist, in mice and rats. Biochem Pharmacol *34*, 1279-1285.
Shearin, A.L., Monks, B.R., Seale, P., and Birnbaum, M.J. (2016). Lack of AKT in adipocytes causes severe lipodystrophy. Mol Metab *5*, 472-479.
Small, L., Ehrlich, A., Iversen, J., Ashcroft, S.P., Trost, K., Moritz, T., Hartmann, B., Holst, J.J., Treebak, J.T., Zierath, J.R.*, et al.* (2022). Comparative analysis of oral and intraperitoneal glucose tolerance tests in mice. Mol Metab *57*, 101440.
Solinas, G., and Becattini, B. (2022). PI3K and AKT at the Interface of Signaling and Metabolism. Curr Top Microbiol Immunol *436*, 311-336.
Stein, D.T., Esser, V., Stevenson, B.E., Lane, K.E., Whiteside, J.H., Daniels, M.B., Chen, S., and McGarry, J.D. (1996). Essentiality of circulating fatty acids for glucose-stimulated insulin secretion in the fasted rat. J Clin Invest *97*, 2728-2735.
Titchenell, P.M., Lazar, M.A., and Birnbaum, M.J. (2017). Unraveling the Regulation of Hepatic Metabolism by Insulin. Trends Endocrinol Metab *28*, 497-505.
Titchenell, P.M., Quinn, W.J., Lu, M., Chu, Q., Lu, W., Li, C., Chen, H., Monks, B.R., Chen, J., Rabinowitz, J.D.*, et al.* (2016). Direct Hepatocyte Insulin Signaling Is Required for Lipogenesis but Is Dispensable for the Suppression of Glucose Production. Cell Metab *23*, 1154-1166.

Trayhurn, P., Thomas, M.E., Duncan, J.S., and Rayner, D.V. (1995). Effects of fasting and refeeding on ob gene expression in white adipose tissue of lean and obese (oblob) mice. FEBS Lett *368*, 488-490.

van Vliet, S., Koh, H.E., Patterson, B.W., Yoshino, M., LaForest, R., Gropler, R.J., Klein, S., and Mittendorfer, B. (2020). Obesity Is Associated With Increased Basal and Postprandial beta-Cell Insulin Secretion Even in the Absence of Insulin Resistance. Diabetes *69*, 2112-2119.

von Mehren, M., George, S., Heinrich, M.C., Schuetze, S.M., Yap, J.T., Yu, J.Q., Abbott, A., Litwin, S., Crowley, J., Belinsky, M.*, et al.* (2020). Linsitinib (OSI-906) for the Treatment of Adult and Pediatric Wild-Type Gastrointestinal Stromal Tumors, a SARC Phase II Study. Clin Cancer Res *26*, 1837-1845.

Yoshida, T. (1992). The antidiabetic beta 3-adrenoceptor agonist BRL 26830A works by release of endogenous insulin. Am J Clin Nutr *55*, 237S-241S.

Figure 1. Adipocyte AKT signaling in-vivo depends on PI3Kα and PI3Kβ. (**A**) Growth curves of PI3Kα^{AdQ} and PI3K$\alpha^{F/F}$ mice. (**B**) Fed serum free fatty acids (FFA) of the mice above. (**C**) Fasting serum FFA, fasting blood glucose, and fasting serum insulin of PI3Kα^{AdQ} and PI3K$\alpha^{F/F}$ mice. (**D**) adipose tissues weights of PI3Kα^{AdQ} and PI3K$\alpha^{F/F}$ mice. (**E-F**) Adipocyte size distribution of and histology of epidydimal fat pads. (**G**) In-vivo pharmacological mapping of the PI3K isoforms driving AKT signaling in the adipocyte in PI3Kα^{AdQ} and PI3K$\alpha^{F/F}$ mice fasted for 12 hours and sacrificed 10 minutes after i.p. injection of 2 g/Kg of glucose with either vehicle or the indicated PI3K inhibitor: 6 mg/Kg for TGX221, IPI549, GSK2636771, and 12 mg/Kg for PIK294. (**H**) The effect of TGX221 and GSK2636771 on AKT phosphorylation was evaluated in PI3K$\alpha^{F/F}$ control mice. Scale bar 100 μm for F. n=7 mice PI3K$\alpha^{F/F}$ and n=6 mice PI3Kα^{AdQ} for A-D, n=6 mice for E-F, 3-6 mice for G, and 3 mice for H. Data are mean ± s.e.m. Statistical analysis was performed using Mann-Whitney for C or unpaired t-test for G.

Figure 2. Adipocyte PI3K activity links adipostasis with insulin secretion through an adipoincretin effect. (**A**) Blood glucose was measured in PI3Kα^{AdQ} and PI3K$\alpha^{F/F}$ mice fasted overnight for 12 hours and injected i.p. with 2 g/Kg of glucose with either vehicle or 6 mg/Kg of the PI3Kβ-selective inhibitor GSK2636771. (**B**) Serum FFA; (**C**) serum insulin; and (**D**) serum C-peptide of the mice from A. (**E-F**) immunoblot analysis of AKT phosphorylation in adipose tissue, liver, and muscle from mice as from A one-hour post-injection. n=6 for A-D, n=2-5 for E (2 for fasting), n=5 for F. Data are represented as mean ± s.e.m. Statistical analysis was performed using repeated measures two-way ANOVA for A-D and Mann-Whitney for F. Indicated P-values in B-D are the most conservative for PI3Kα^{AdQ} + Glucose + GSK2636771 vs PI3Kα^{AdQ} +Glucose, or vs PI3K$\alpha^{F/F}$ + Glucose + GSK2636771.

Figure 3. The adipoincretin effect operates in fed and fasted mice independently from glucose administration. (**A**) Blood glucose of fed PI3Kα^{AdQ} and PI3K$\alpha^{F/F}$ mice injected with 6 mg/Kg of GSK2636771. (**B**) Serum levels of FFA; (**C**) insulin; and (**D**) C-peptide of the mice from A. (**E**) Blood glucose of mice as from A but injected with 6 mg/Kg of GSK2636771 after 12 hours of fasting. (**F**) Serum levels of FFA; (**G**) insulin; and (**H**) leptin of the mice from E. n=5 mice for A-D and n=6 mice for E-H. Data are mean ± s.e.m. Statistical analysis was performed using repeated measures, two-way ANOVA, and unpaired t-test for H.

Figure 4. The hyperinsulinemia induced by systemic PI3K inhibition and the adipoincretin effect are partially dependent on lipolysis. (**A**) Blood glucose of 12 hours fasted C57Bl/6 wild-type mice after injection of 8 mg/kg of Buparlisib in the presence or absence of 100 mg/kg of nicotinic acid. (**B**) Serum abundance of FFA and (**C**) insulin from the mice above. (**D**) Blood glucose of 12 hours fasted C57Bl/6 wild-type mice after injection of 3.5 mg/kg of Taselisib in the presence or absence of 100 mg/kg of nicotinic acid. (**E**) The abundance of serum FFA and (**F**) serum insulin from the mice in D. (**G**) Blood glucose of 12 hours fasted PI3Kα^{AdQ} mice after injection of 6 mg/kg of GSK2636771 in the presence or absence of 100 mg/kg of nicotinic acid. (**H**) The abundance of serum FFA and of (**I**) serum insulin from the mice in G. n=5 mice for A-C and n=6 for D-F, G-H: n=6 GSK2636771 and n=5 for GSK2636771 with NA. Data are mean ± s.e.m. Statistical analysis was performed using repeated measures two-way ANOVA and Mann-Whitney for insulin AUC.

Figure 5. The adipoincretin effect is associated with reduced BCAA and increased 3OH-4C-Carnitine. (**A**) Plasma abundance of C-peptide in 12 hours fasted PI3Kα^{AdQ} and PI3K$\alpha^{F/F}$ after injection of 6 mg/kg of GSK2636771. (**B**) Blood glucose of the mice in A**.** (**C**) Plasma abundance of glutamine; (**D**) branched-chain amino acids (BCAA) and (**E**) branched-chain ketoacids (BCKA) from the mice in A**.** (**F**) Plasma levels of free carnitine and acyl-carnitines in the mice from above. N= 10 mice. Data are mean ± s.e.m. Statistical analysis was performed using repeated measures two-way ANOVA and Šídák's multiple comparisons test for B.

Figure 6. An adipostat paradigm for the insulin system. During feeding, insulin secretion is governed mainly by the feedforward action of the glucoincretin effect and, to a lesser extent, by the cephalic phase of insulin secretion and increased blood glucose (right part of the model shaded in green). During fasting (the left part of the model shaded in red), the glucoincretin effect and cephalic phase are absent, and blood glucose concentration is minimal. In these conditions, insulin secretion is mainly governed by a closed-loop feedback control system mediated by insulin-PI3K signaling in the adipocyte. The system can be regarded as an adipostat, a "cruise control" for lipolysis where adipocyte PI3K activity links lipolysis with basal insulin secretion through the adipoincretin effect.

Figure 1

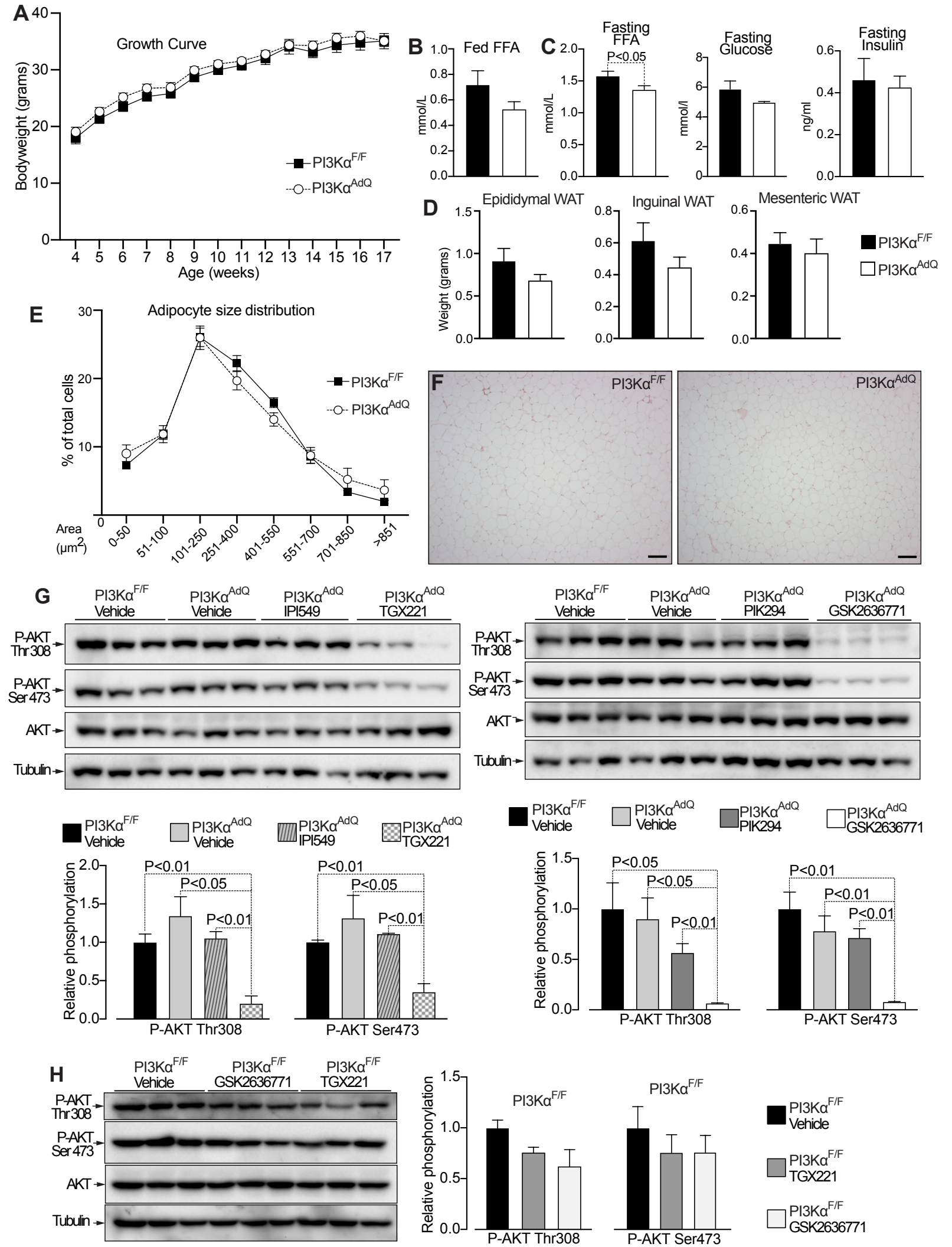
A
Growth Curve
Bodyweight (grams)
Age (weeks)
PI3Kα F/F
PI3Kα AdQ
B
Fed FFA
mmol/L
C
Fasting FFA
P<0.05
Fasting Glucose
Fasting Insulin
ng/ml
D
Epididymal WAT
Inguinal WAT
Mesenteric WAT
Weight (grams)
E
Adipocyte size distribution
% of total cells
Area (μm2)
0-50
51-100
101-250
251-400
401-550
551-700
701-850
>851
F
G
PI3Kα F/F Vehicle
PI3Kα AdQ Vehicle
PI3Kα AdQ IPI549
PI3Kα AdQ TGX221
PI3Kα AdQ PIK294
PI3Kα AdQ GSK2636771
P-AKT Thr308
P-AKT Ser473
AKT
Tubulin
Relative phosphorylation
P<0.01
P<0.05
H
PI3Kα F/F GSK2636771
PI3Kα F/F TGX221

Figure 2

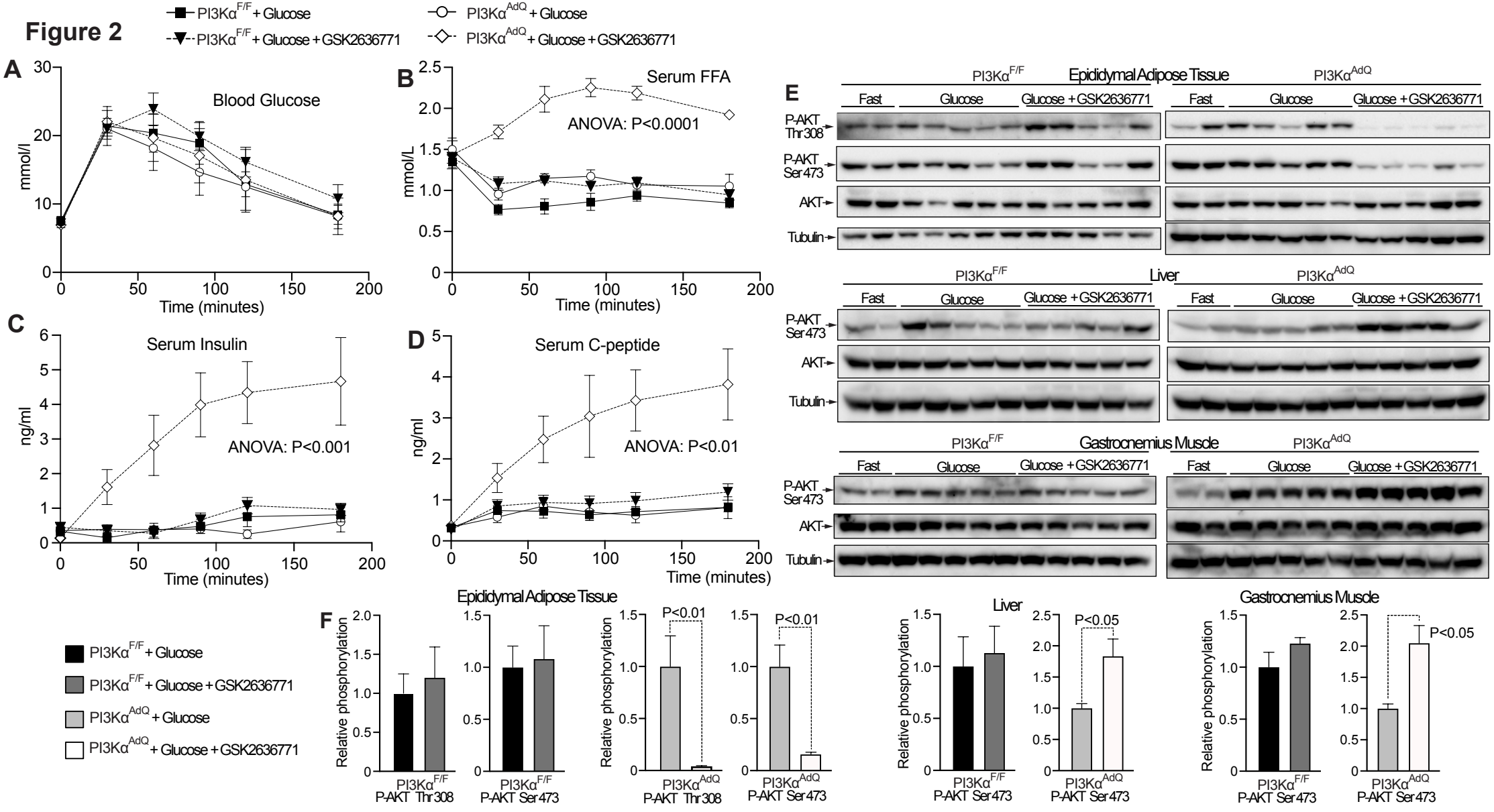
PI3Kα F/F + Glucose
PI3Kα F/F + Glucose + GSK2636771
PI3Kα AdQ + Glucose
PI3Kα AdQ + Glucose + GSK2636771
A
Blood Glucose
mmol/l
Time (minutes)
B
Serum FFA
ANOVA: P<0.0001
mmol/L
Time (minutes)
C
Serum Insulin
ANOVA: P<0.001
ng/ml
Time (minutes)
D
Serum C-peptide
ANOVA: P<0.01
ng/ml
Time (minutes)
E
Epididymal Adipose Tissue
Liver
Gastrocnemius Muscle
Fast
Glucose
Glucose + GSK2636771
P-AKT Thr308
P-AKT Ser473
AKT
Tubulin
F
Relative phosphorylation
P<0.01
P<0.05
PI3Kα F/F + Glucose
PI3Kα F/F + Glucose + GSK2636771
PI3Kα AdQ + Glucose
PI3Kα AdQ + Glucose + GSK2636771

Figure 3

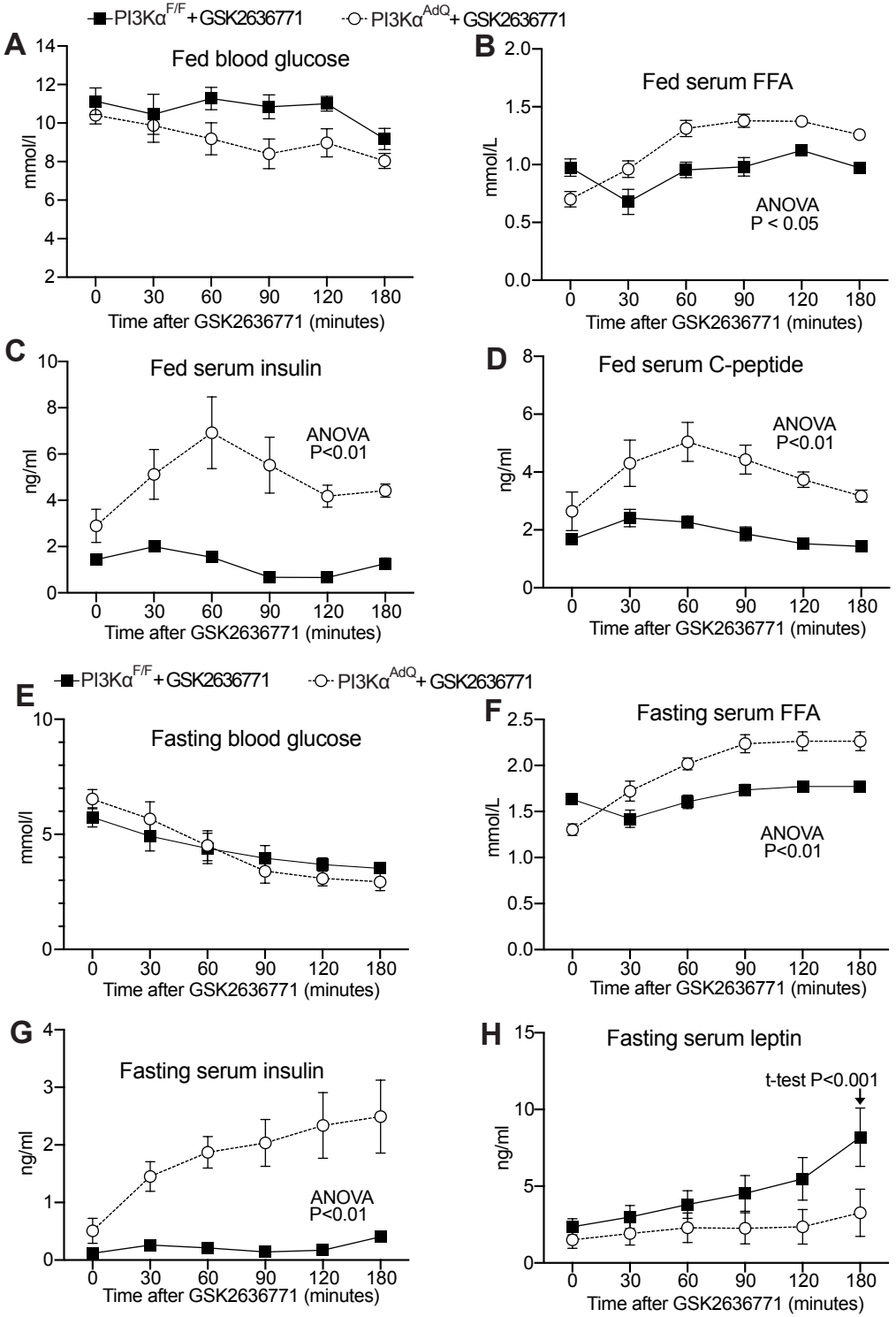
PI3Kα F/F + GSK2636771
PI3Kα AdQ + GSK2636771
A
Fed blood glucose
mmol/l
Time after GSK2636771 (minutes)
B
Fed serum FFA
mmol/L
ANOVA
P < 0.05
Time after GSK2636771 (minutes)
C
Fed serum insulin
ng/ml
ANOVA
P<0.01
Time after GSK2636771 (minutes)
D
Fed serum C-peptide
ng/ml
ANOVA
P<0.01
Time after GSK2636771 (minutes)
E
Fasting blood glucose
mmol/l
Time after GSK2636771 (minutes)
F
Fasting serum FFA
mmol/L
ANOVA
P<0.01
Time after GSK2636771 (minutes)
G
Fasting serum insulin
ng/ml
ANOVA
P<0.01
Time after GSK2636771 (minutes)
H
Fasting serum leptin
t-test P<0.001
ng/ml
Time after GSK2636771 (minutes)

Figure 4

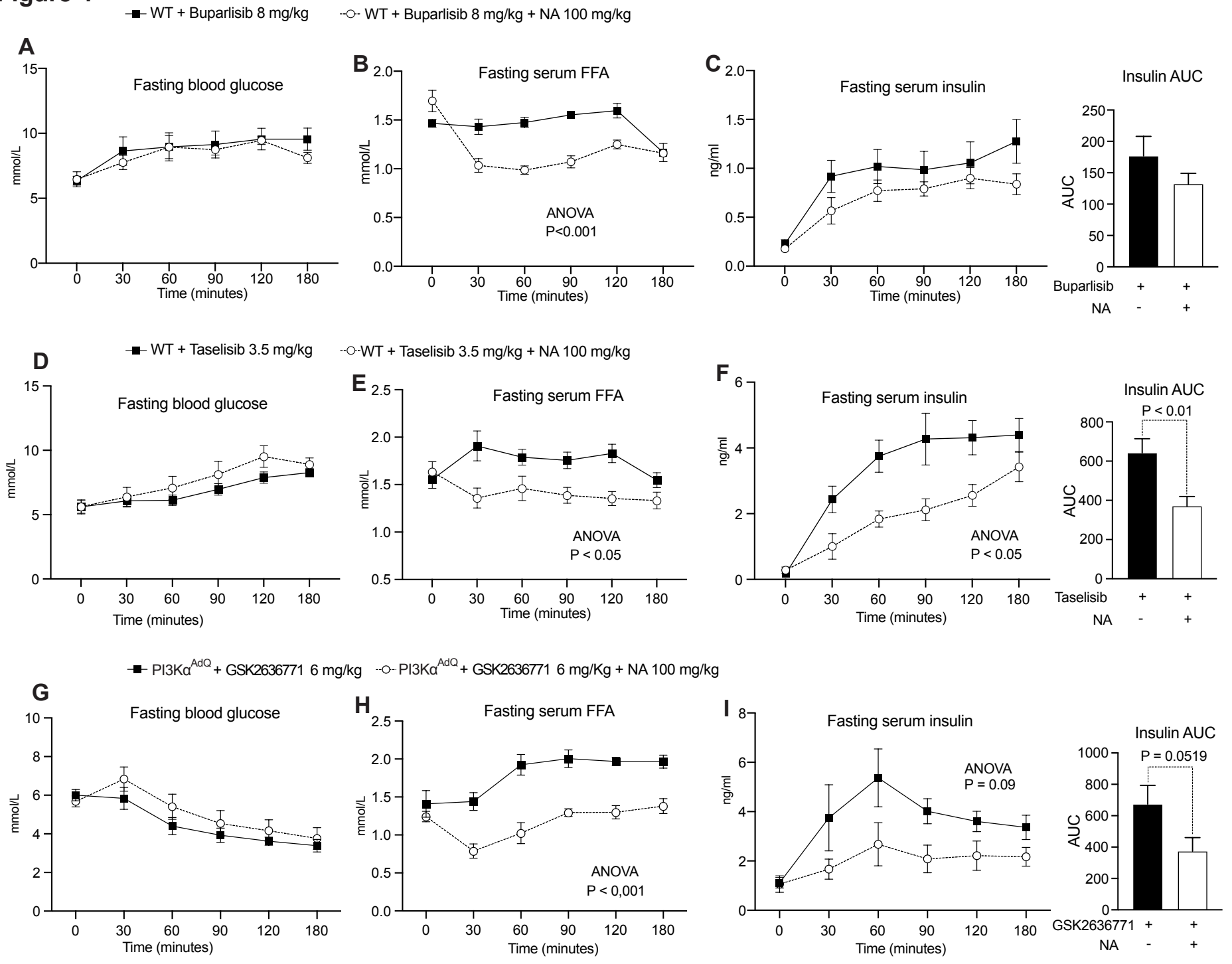
WT + Buparlisib 8 mg/kg
WT + Buparlisib 8 mg/kg + NA 100 mg/kg
A
Fasting blood glucose
mmol/L
Time (minutes)
B
Fasting serum FFA
ANOVA
P<0.001
C
Fasting serum insulin
ng/ml
Insulin AUC
AUC
Buparlisib + +
NA - +
WT + Taselisib 3.5 mg/kg
WT + Taselisib 3.5 mg/kg + NA 100 mg/kg
D
E
ANOVA
P < 0.05
F
ANOVA
P < 0.05
P < 0.01
Taselisib + +
NA - +
PI3Kα^AdQ + GSK2636771 6 mg/kg
PI3Kα^AdQ + GSK2636771 6 mg/Kg + NA 100 mg/kg
G
H
ANOVA
P < 0,001
I
ANOVA
P = 0.09
P = 0.0519
GSK2636771 + +
NA - +

Figure 5

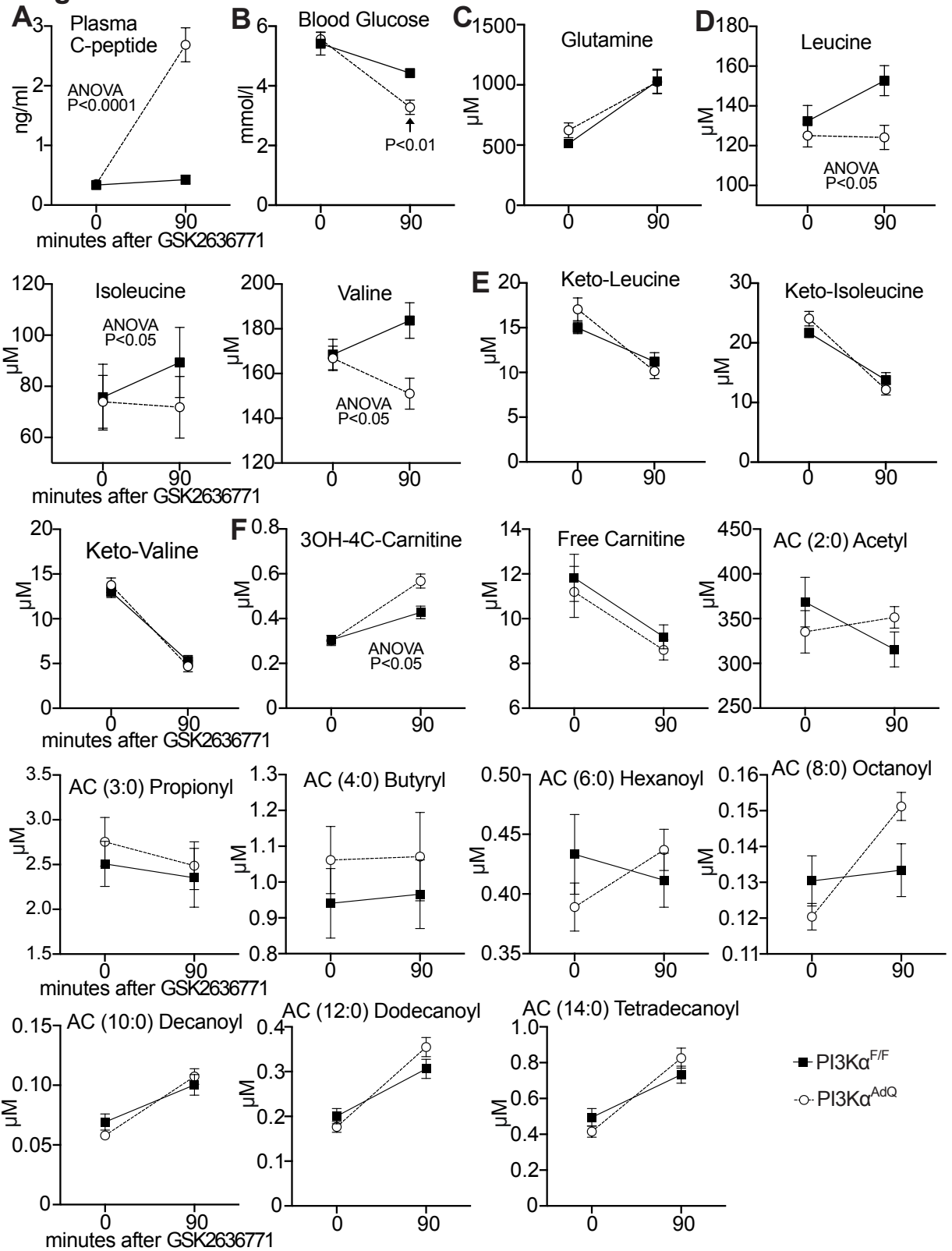
A
Plasma C-peptide
ng/ml
ANOVA P<0.0001
B
Blood Glucose
mmol/l
P<0.01
C
Glutamine
μM
D
Leucine
μM
ANOVA P<0.05
minutes after GSK2636771
Isoleucine
μM
ANOVA P<0.05
Valine
μM
ANOVA P<0.05
E
Keto-Leucine
μM
Keto-Isoleucine
μM
minutes after GSK2636771
Keto-Valine
μM
F
3OH-4C-Carnitine
μM
ANOVA P<0.05
Free Carnitine
μM
AC (2:0) Acetyl
μM
minutes after GSK2636771
AC (3:0) Propionyl
μM
AC (4:0) Butyryl
μM
AC (6:0) Hexanoyl
μM
AC (8:0) Octanoyl
μM
minutes after GSK2636771
AC (10:0) Decanoyl
μM
AC (12:0) Dodecanoyl
μM
AC (14:0) Tetradecanoyl
μM
minutes after GSK2636771
PI3Kα F/F
PI3Kα AdQ

Figure 6

The insulin-adipostat control system

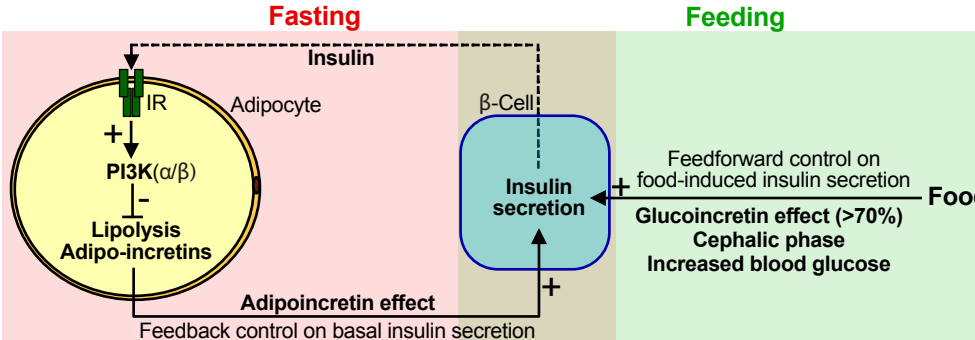

Supplemental information for:

Adipocyte PI3K links adipostasis with insulin secretion through an adipoincretin effect

Barbara Becattini[1], Angela Molinaro[1,2], Marcus Henricsson[1], Jan Borén[1], and Giovanni Solinas[1*]

1 Department of Molecular and Clinical Medicine, Institute of Medicine, University of Gothenburg, Gothenburg, Sweden.

2 Present address: Department of Laboratory Medicine, Institute of Medicine, University of Gothenburg, Gothenburg, Sweden.

[*]Correspondence: giovanni.solinas@wlab.gu.se

Seven supplemental figures.

Fig. S1

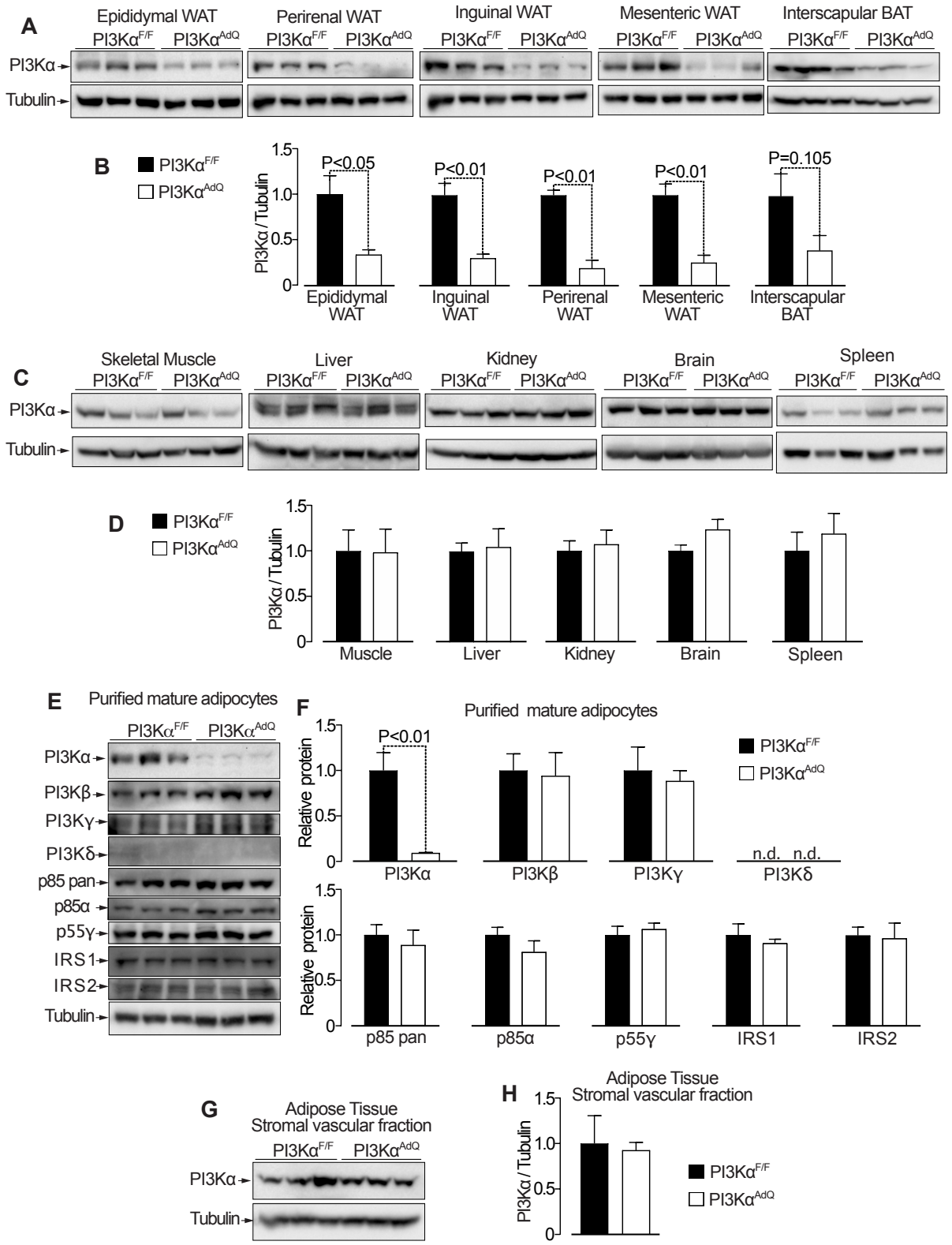
A
Epididymal WAT
Perirenal WAT
Inguinal WAT
Mesenteric WAT
Interscapular BAT
PI3Kα F/F
PI3Kα AdQ
PI3Kα
Tubulin
B
PI3Kα F/F
PI3Kα AdQ
PI3Kα / Tubulin
P<0.05
P<0.01
P<0.01
P<0.01
P=0.105
Epididymal WAT
Inguinal WAT
Perirenal WAT
Mesenteric WAT
Interscapular BAT
C
Skeletal Muscle
Liver
Kidney
Brain
Spleen
D
Muscle
Liver
Kidney
Brain
Spleen
E
Purified mature adipocytes
PI3Kβ
PI3Kγ
PI3Kδ
p85 pan
p85α
p55γ
IRS1
IRS2
F
Purified mature adipocytes
Relative protein
n.d.
G
Adipose Tissue
Stromal vascular fraction
H
Adipose Tissue
Stromal vascular fraction

Figure S1. Efficient and specific PI3Kα deletion in PI3Kα^{AdQ} mice, related to Figure 1.

(**A**) PI3Kα^{AdQ} and PI3Kα$^{F/F}$ mice from Figure 1 were sacrificed, and PI3Kα protein abundance in their adipose tissue pads was measured by immunoblotting. (**B**) Quantification of the immunoblots in A. (**C**) PI3Kα protein abundance in muscle, liver, kidney, brain, and spleen was measured by immunoblotting. (**D**) Quantification of the immunoblots in C. (**E**) The abundances of class-1 PI3K catalytic and adapter subunits and of the insulin receptor substrates IRS1 and IRS2 were quantified by immunoblot in mature adipocytes purified from epididymal fat pads. (**F**) Quantification of the immunoblots in E. (**G**) Immunoblot analysis of PI3Kα protein abundance in the stromal vascular fractions of the epididymal fat pads in E. (**H**) Quantification of the immunoblots in G.

n=3 mice per group for A-D and G-H, n=6 for E-F (n=3 for IRS1 and IRS2).

Data are mean ± s.e.m. Statistical analysis was performed using the unpaired t-test or Mann-Whitney for E (n=6).

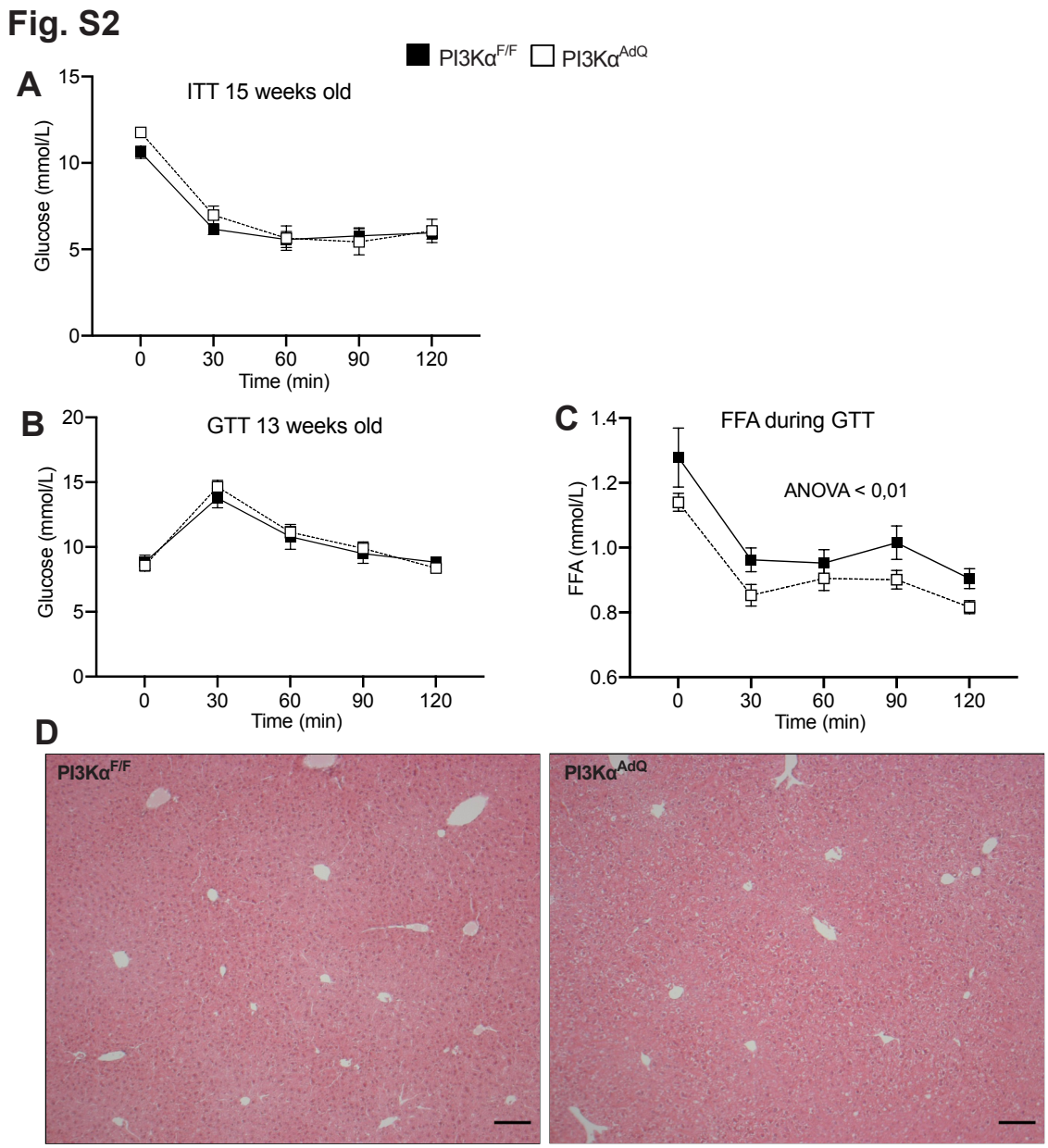

Figure S2. PI3Kα^{AdQ} mice display normal glucose and lipid control, related to Figure 1. (**A**) Insulin tolerance test (ITT): PI3Kα^{AdQ} and PI3Kα$^{F/F}$ mice were fasted for 4 hours, and blood glucose was measured at the indicated time points after i.p. injection of 1 IU/kg of insulin. (**B**) Glucose tolerance test (GTT): PI3Kα^{AdQ} and PI3Kα$^{F/F}$ mice were fasted for 4 hours, and blood glucose was measured at the indicated time points after i.p. injection of 1 g/kg of glucose. (**C**) Quantification of serum-free fatty acids during the GTT. (**D**) Representative image of liver histology. Scale bar 100 μm. n=6 mice per group, data are mean ± s.e.m. Statistical analysis was performed using repeated measures two-way ANOVA.

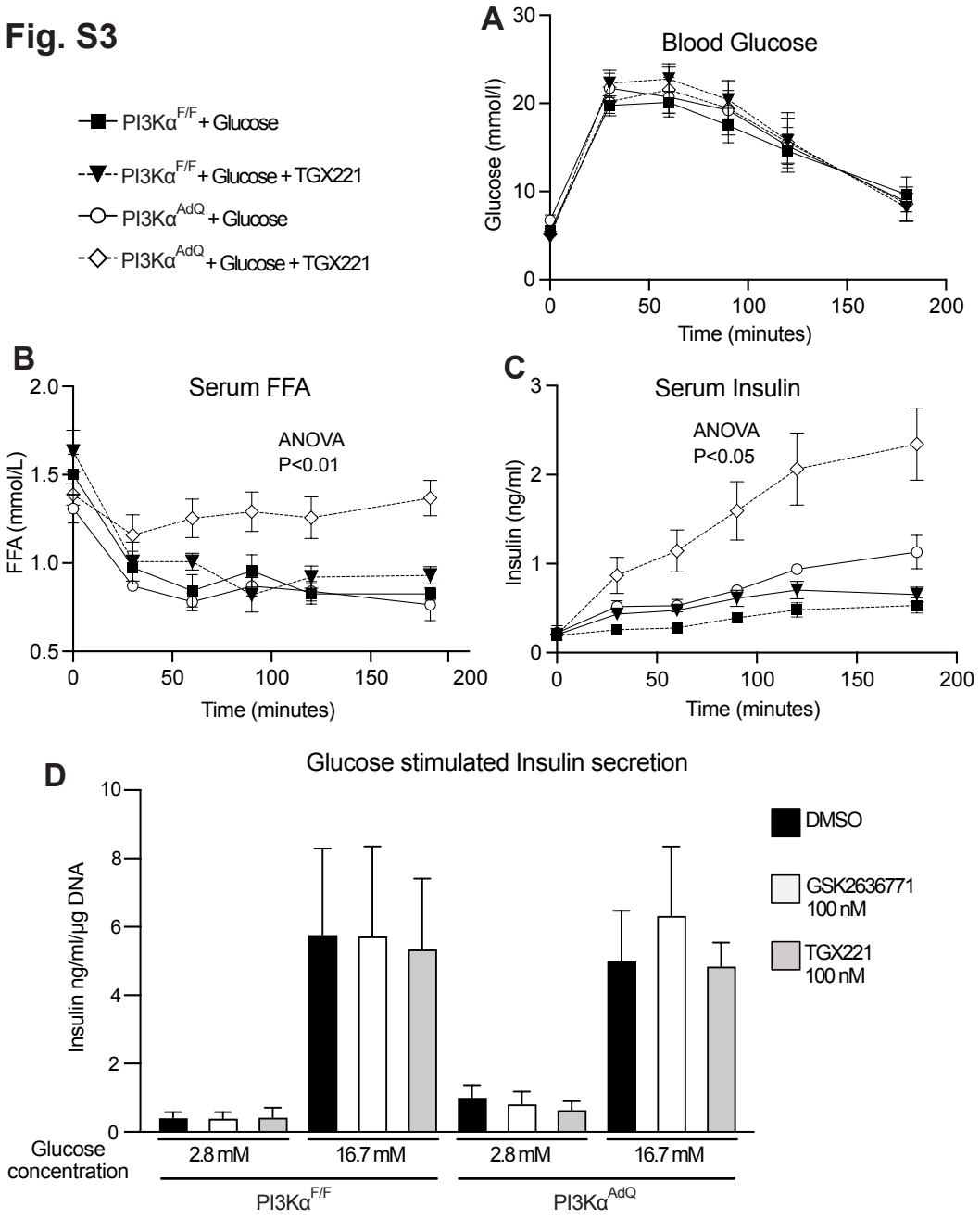

Figure S3. Adipocyte PI3K activity links adipostasis with insulin secretion through an adipoincretin effect, related to Figure 2.

(**A**) PI3Kα^{AdQ} and PI3K$\alpha^{F/F}$ mice were fasted for 12 hours and injected i.p. with 2 g/Kg of glucose with either vehicle or 8 mg/Kg of the PI3Kβ-selective inhibitor TGX221. Blood glucose was measured at the indicated time points. (**B**) Serum FFA, and (**C**) serum insulin of the mice from

A. (**D**) Glucose stimulated insulin secretion of islets isolated from PI3Kα^{AdQ} and PI3K$\alpha^{F/F}$ mice kept in the presence of either vehicle, the PI3Kβ-selective inhibitors GSK2636771 or TGX221. n=6 mice per group in A-C and n=3 for D. Data are mean ± s.e.m. Statistical analysis was performed using repeated measures two-way ANOVA for A-C and unpaired t-test for D. For B, glucose significantly reduced FFA levels in all groups except for PI3Kα^{AdQ} mice co-treated with TGX221. The P-value in B is for PI3Kα^{AdQ} + Glucose + TGX221 vs PI3Kα^{AdQ} +Glucose. C, the indicated P-value is the most conservative for the following comparisons for PI3Kα^{AdQ} + Glucose + TGX221 vs. PI3Kα^{AdQ} + Glucose, and PI3Kα^{AdQ} + Glucose + TGX221 vs. PI3K$\alpha^{F/F}$ + Glucose + TGX221.

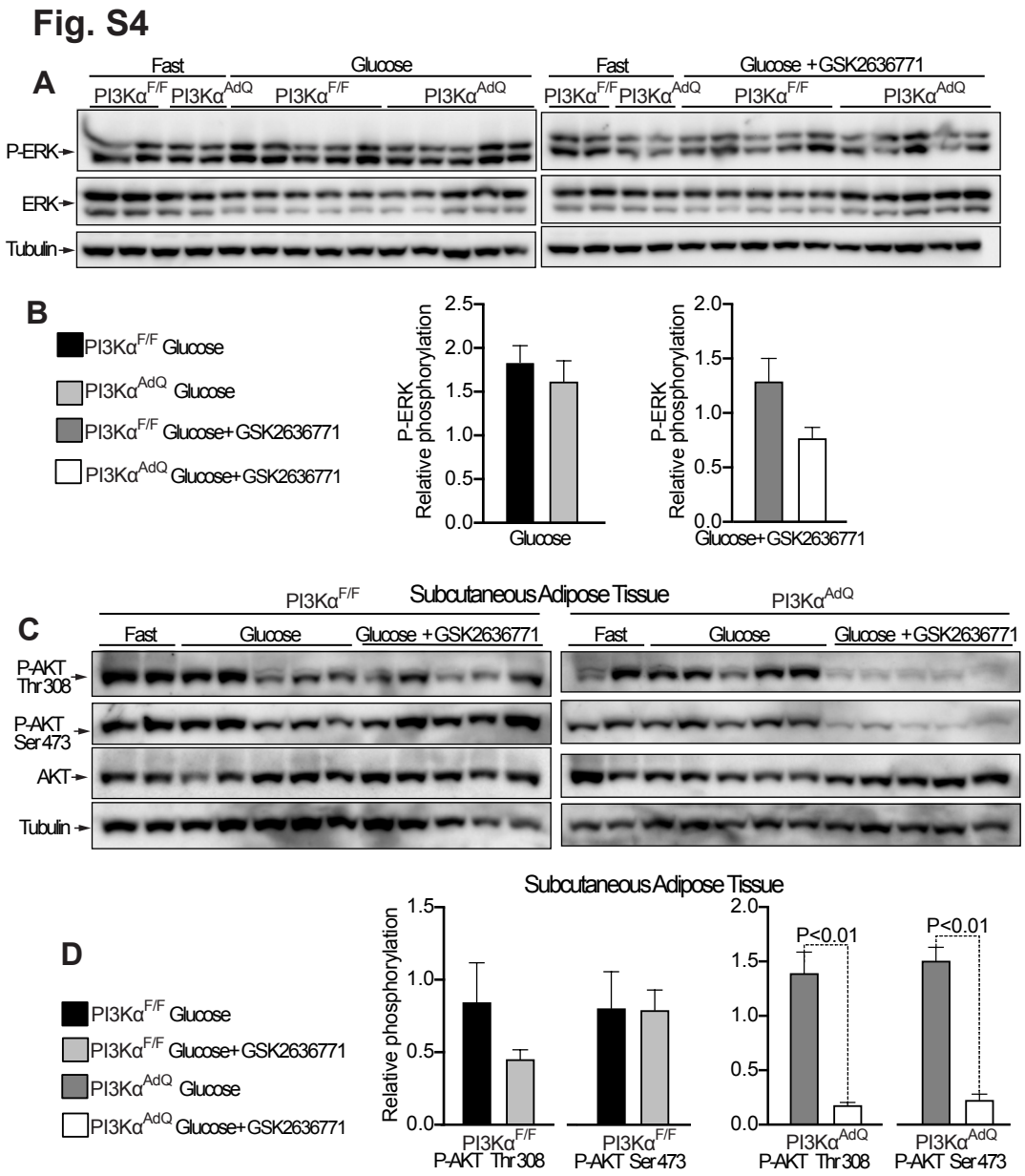

Figure S4. Effects of adipose tissue-selective inhibition on ERK and AKT phosphorylation in fat tissues, related to Figure 2.

(**A**) Immunoblot analysis of ERK phosphorylation in the epidydimal adipose tissues from PI3Kα^{AdQ} and PI3K$\alpha^{F/F}$ mice described in Figure 2. (**B**) Quantification of the immunoblots in A. (**C**) Immunoblot analysis of AKT phosphorylation in the subcutaneous inguinal adipose tissues from PI3Kα^{AdQ} and PI3K$\alpha^{F/F}$ mice described in Figure 2. (**D**) Quantification of the immunoblots in C. n=2-5 mice per group, Data are mean ± s.e.m. Statistical analysis was performed using the Mann–Whitney test.

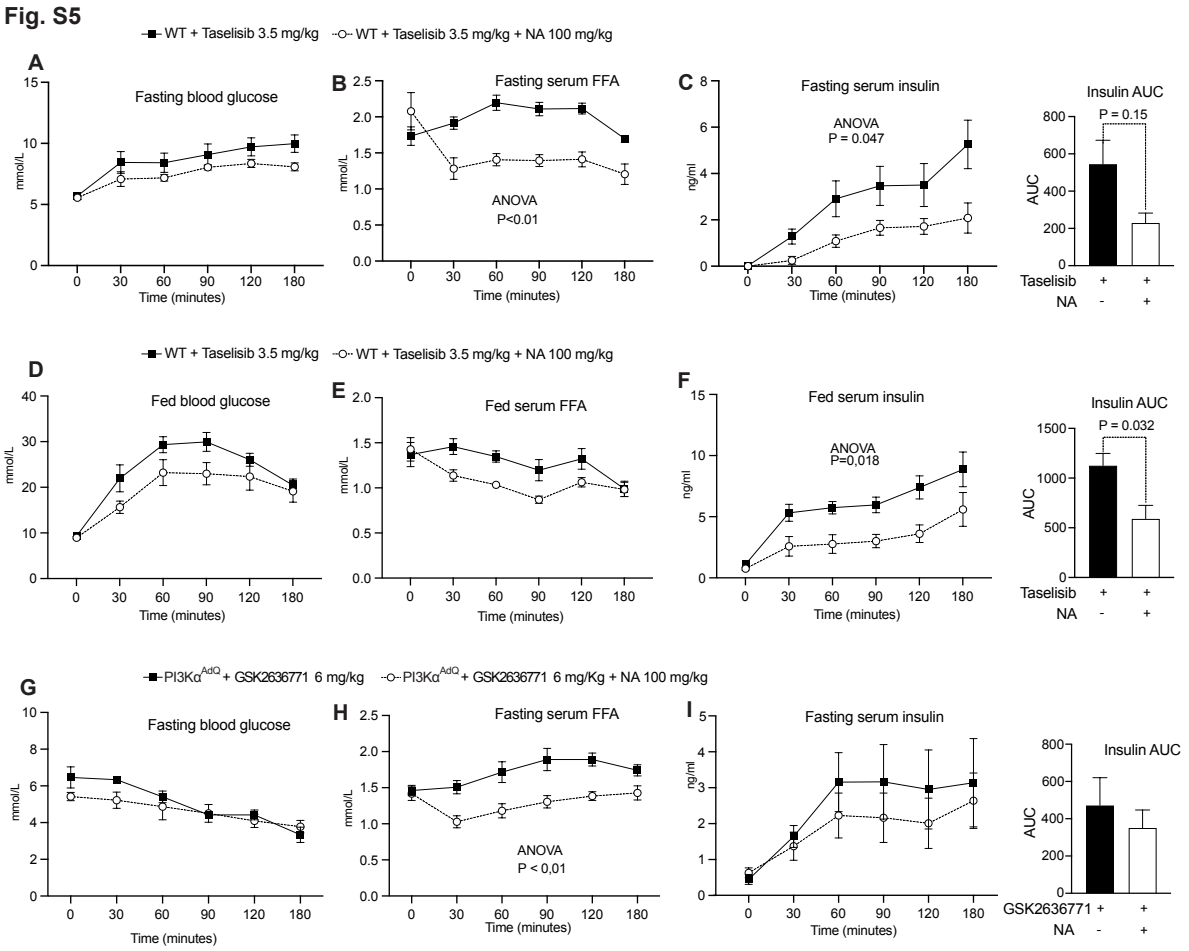

Figure S5. The hyperinsulinemia induced by systemic PI3K inhibition and the adipoincretin effect are partially dependent on lipolysis, related to Figure 4.

Wild-type C57BL/6 mice were fasted for 12 hours and injected with pan-PI3K inhibitor Taselisib in the presence or absence of nicotinic acid (NA). (**A**) Blood glucose, (**B**) serum FFA, (**C**) serum insulin of the mice above. The same C57BL/6 mice above were kept in fed conditions and injected with pan-PI3K inhibitor Taselisib in the presence or absence of nicotinic acid (NA). (**D**) Blood glucose, (**E**) serum FFA, (**F**) serum insulin of the mice above.

PI3Kα^{AdQ} mice were fasted for 12 hours and injected with GSK2636771, and one group of PI3Kα^{AdQ} received GSK263771 together with nicotinic acid (NA). (**G**) Blood glucose, (**H**) serum FFA, (**I**) serum insulin of the mice above.

n=5 mice for A-F and for G-H: n=5 GSK2636771 and n=6 for GSK2636771 with NA.

Data are mean ± s.e.m. Statistical analysis was performed using repeated measures two-way ANOVA and Mann-Whitney for insulin AUC.

Fig. S6

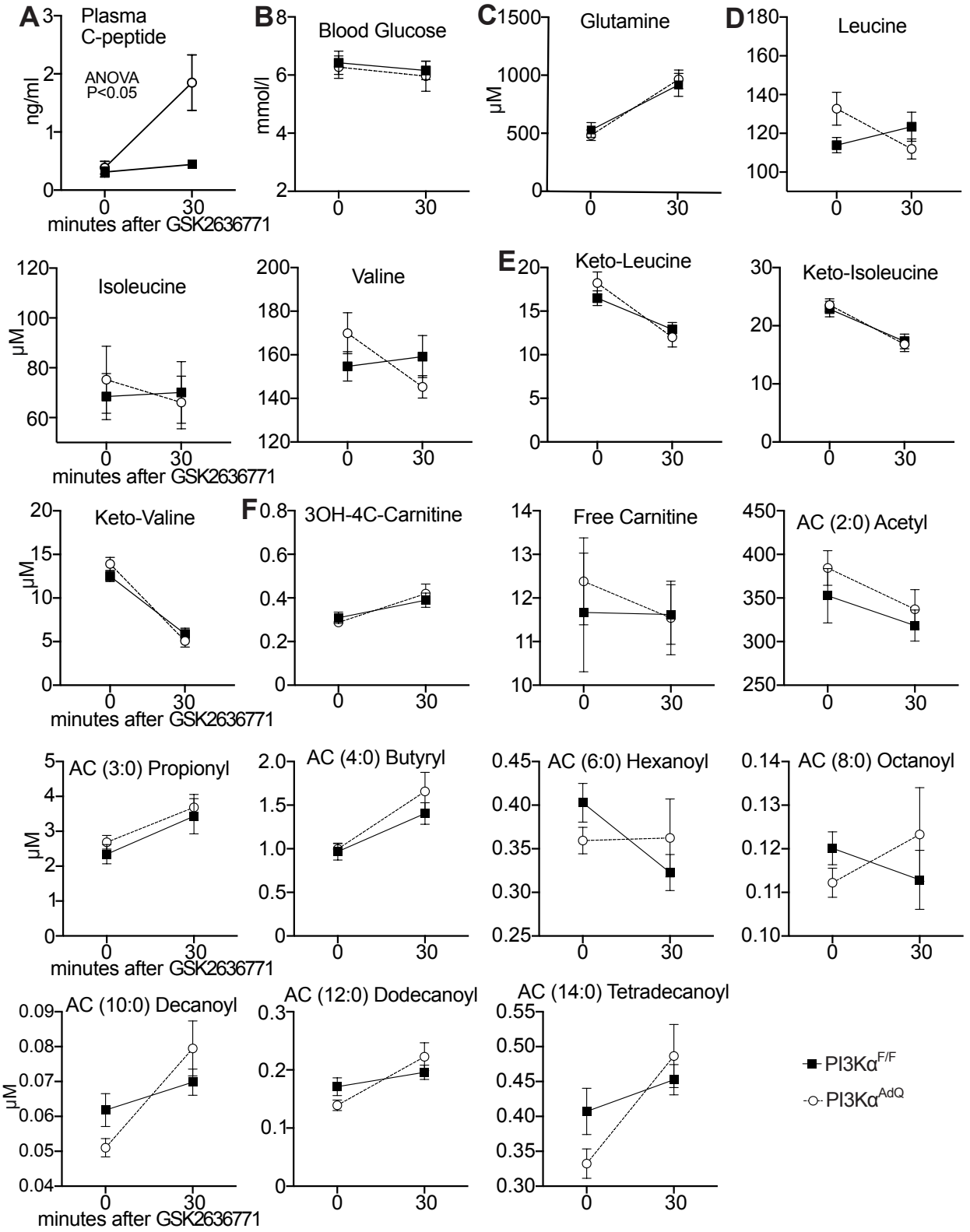
A
Plasma C-peptide
ANOVA P<0.05
ng/ml
minutes after GSK2636771
B
Blood Glucose
mmol/l
C
Glutamine
μM
D
Leucine
Isoleucine
Valine
E
Keto-Leucine
Keto-Isoleucine
Keto-Valine
F
3OH-4C-Carnitine
Free Carnitine
AC (2:0) Acetyl
AC (3:0) Propionyl
AC (4:0) Butyryl
AC (6:0) Hexanoyl
AC (8:0) Octanoyl
AC (10:0) Decanoyl
AC (12:0) Dodecanoyl
AC (14:0) Tetradecanoyl
PI3Kα F/F
PI3Kα AdQ

Figure S6. Targeted metabolomics, related to Figure 5.

PI3Kα^{AdQ} and PI3K$\alpha^{F/F}$ mice fasted for 12 hours and were injected with GSK2636771, and plasma was collected at 0 minutes (before GSK2636771 injection) and at 30 minutes post-injection. Plasma levels of (**A**) C-peptide, (**B**) glucose, (**C**) glutamine, (**D**) branched-chain amino acids, (**E**) ketoacids, and (**F**) acylcarnitines were measured.

n=10 mice. Data are mean ± s.e.m. Statistical analysis was performed using repeated measures two-way ANOVA.

Fig. S7

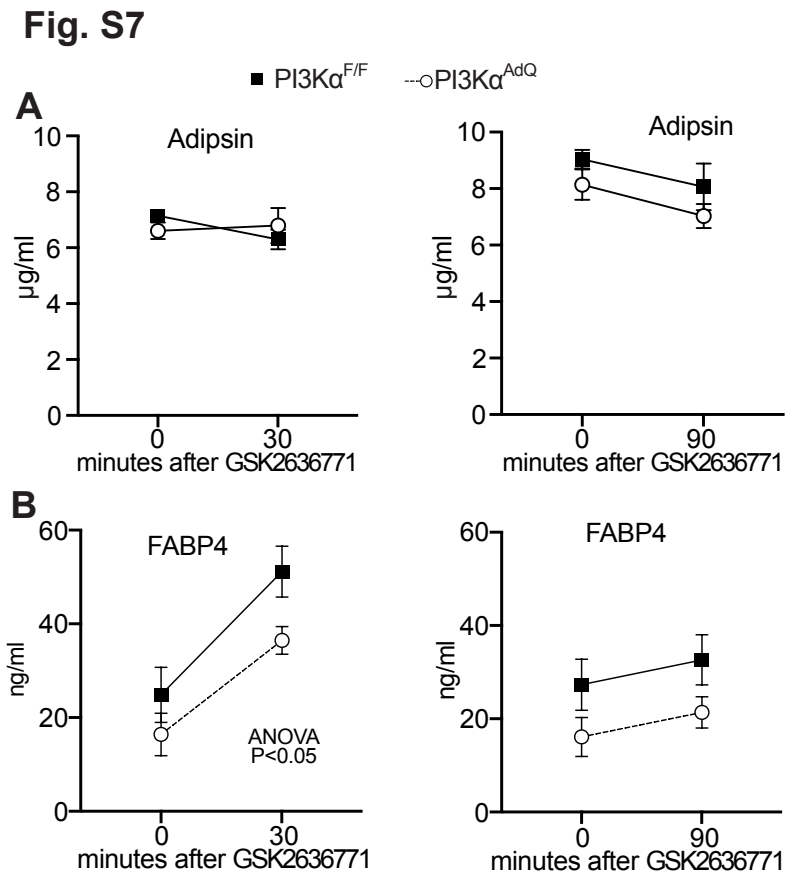

Figure S7. The adipoincretin effect is not associated with plasma abundances of Adipsin and FABP4, related to Figure 5.

PI3Kα^{AdQ} and PI3K$\alpha^{F/F}$ mice were fasted for 12 hours, and injected with GSK2636771, and plasma was collected at 0 minutes (before GSK2636771 injection) and at 30 minutes post-injection or, in another cohort, at 0' (before GSK2636771 injection) and at 90 minutes post-injection. Plasma levels of (**A**) Adipsin and (**B**) FABP4 were measured by ELISA.

n=7 mice for A and n=9 mice for B. Data are mean ± s.e.m. Statistical analysis was performed using repeated measures two-way ANOVA. P value in B refers to an effect of GSK2636771 independent from the genotype.

METHODS

KEY RESOURCES TABLE

REAGENT or RESOURCE	SOURCE	IDENTIFIER
Antibodies		
AKT Phospho (Thr308)	Cell Signaling	4056
AKT Phospho (Ser373) XP	Cell Signaling	4060
AKT	Cell Signaling	9272
Erk 1/2 (p44/42 MAPK) Phospho(Thr202/Tyr204) XP	Cell Signaling	9101
Erk 1/2 (p44/42 MAPK)	Cell Signaling	9102
IRS1	Millipore	06248
IRS2	Millipore	MAB515
PI3K p85	Cell Signaling	4257S
PI3K p85α	Abcam	Ab133595
PI3K p55γ	Abcam	Ab238509
Tubulin α/β	Cell Signaling	2148S
PI3Kα	Cell Signaling	4249
PI3Kβ	Cell Signaling	3011
PI3Kδ	Millipore	04-401
PI3Kγ	a gift of Prof. Matthias Wymann University of Basel	(Russian)
Chemicals, Peptides, Recombinant Proteins and Inhibitors		
Insulin	Humalog Lilly	VL7510
Glucose	Acros	410955000
BSA	Fisher Scientific	BP9702
ECL-anti rabbit IgG HRP	GE Healthcare	NA934V
ECL-anti mouse IgG HRP	GE Healthcare	LNA931V
Collagenase P	Roche	11213865001
GSK2636771 (Inhibitor PI3Kβ)	SelleckChem	S8002
TGX-221 (Inhibitor PI3Kβ)	MedChem Express	HY-10114
IPI549 (Inhibitor PI3Kγ)	MedChem Express(SelleckChem)	HY-100716
PIK294 (Inhibitor PI3Kδ)	MedChem Express	HY-10303
Buparlisib (BKM120, panPI3K inhibitor)	MedChem Express	HY-70063
Taselisib (GDC-0032, panPI3K inhibitor)	MedChem Express	HY-13898
Critical Commercial Assays		
Insulin ELISA Kit	Crystal Chem	90080
C-peptide Elisa Kit	Crystal Chem	90050
FFA (NEFA-HR set)	Fuji Film	436-91995, 434-91795 91096 (standard)
Leptin Elisa Kit	R&D	MOB00B
Adipsin Elisa Kit	R&D	DY5430-05
FABP4 Elisa Kit	BioVendor	RD191036200R
Immobilon Western Chemiluminescence HRP substrate	Millipore	WBKLS0500
Hematoxylin Solution (Mayer's, Modified)	Abcam	AB220365
Eosin	Sigma	HT110116
Experimental Models: Organisms/Strains		

WT	C57BL/6 background	Janvier Labs
PI3Kα^{Flox}	Mixed background	Provided by Victoria Rotter Sopasakis
PI3Kα^{AdQ}	Mixed background	Provided by Victoria Rotter Sopasakis
Software and Algorithms		
Image Lab software (version 5.2.1)	Bio-Rad	http://www.bio-rad.com/en-us/ product/image-lab-software
Graph Pad Prism 7.0	Graph Pad Software	N/A
AxioVision Software	Imaging Sofware	Carl Zeiss Microscopy
Deposited Data		
	Immunoblots images	

CONTACT FOR REAGENT AND RESOURCE SHARING

Further information and requests for reagents may be directed to the Lead Contact, Giovanni Solinas (giovanni.solinas@wlab.gu.se)

Mice and in vivo studies

All mouse studies were approved by the Ethics Committee on Animal Care Use in Gothenburg, Sweden, and were performed according to local regulations. Only male mice were used in this study. Mice were maintained at the EBM specific pathogen-free facility of the University of Gothenburg under a 12-hour light /12-hour dark cycle and at a room temperature of 22°C.

PI3Kα LoxP floxed mice (PI3Kα$^{F/F}$) in 129/SvJ and C57BL/6J mixed background were previously described (Molinaro et al. 2019, PMID: 30982732). PI3Kα^{AdQ} mice and littermate control PI3Kα$^{F/F}$ mice were obtained by crossing Adipoq-Cre mice in pure C57BL/6J background (Jackson labs) with the PI3Kα$^{F/F}$ mice from above. Wild-type (WT) C57BL/6J mice were obtained from Janvier Labs.

For the insulin tolerance test (ITT), mice were fasted for 4 hours and injected intraperitoneally with 1 I.U. of insulin per Kg of body weight. Blood was collected from the tail at the indicated post-injection times, and blood glucose concentrations were measured using a glucometer (Contour Next, Ascensia). For the glucose tolerance test (GTT), mice were fasted for either 4 hours (GTT in Figure S2) or overnight for glucose-mediate suppression of lipolysis (Figure 2) and injected intraperitoneally with either 1 g or 2 g of glucose per Kg of body weight respectively. Blood was collected from the tail at the indicated time points and used to measure blood glucose and prepare serum for measurements of hormones and metabolites.

For in vivo injection of PI3K-selective inhibitors, the indicated dose of the compound was injected intraperitoneally into 8 to 12-months-old PI3Kα^{AdQ} mice and PI3Kα$^{F/F}$ littermate controls or C57BL/6 mice. The injectable solutions of the PI3K inhibitors were freshly prepared as follows: PI3K inhibitor was first dissolved in pure DMSO, and to this master liquid were added one by one and in this order PEG300, Tween 80, and water. The solution was mixed after each addition. The final concentration for the single components is 5% DMSO, 30% PEG, and 1% Tween-80. Control ‘‘vehicle solution’’ was 5% DMSO, 30% PEG, 1% Tween-80, and water. For solutions including nicotinic acid (NA), the NA powder was directly dissolved in the final mix at the desired concentration, and the acidity was adjusted at a value of pH 7 by adding NaOH 1M to the solution.

Blood glucose was measured at the indicated time points after injection, and blood was collected for further measurements of serum insulin, serum FFA, serum leptin, and plasma levels of C-peptide, BCAA, BCKA, free carnitine, and acyl-carnitines.

At sacrifice, mice were anesthetized with isoflurane (Baxter KDG 9623) and euthanized by CO_2 and bleeding.

Insulin, C-peptide, leptin, and adipokines measurements

Insulin and C-peptide levels in serum and plasma were measured using ELISA kits from Crystal Chem. Serum leptin was measured by ELISA kit from R&D. Plasma adipsin (Mouse Complement Factor D) was measured by quantitative sandwich enzyme immunoassay using kits obtained from R&D Systems, and adipocyte FABP4 abundance in plasma was measured using an ELISA kit from BioVendor. All ELISA assays were performed according to the instructions from the manufacturer.

Tissues histology and adipocyte size distribution

Samples of adipose tissue pads and liver were collected from 13-week-old mice. The samples were fixed in 10% formalin, embedded in paraffin, cut into five µm sections, and stained with hematoxylin (Abcam) and eosin (Sigma). H&E stained tissue sections were imaged at 20X magnification with an AxioImager.M1 microscope (Zeiss, Germany). Images of two fields for six mice were analyzed in Fiji using the open-source plugin adiposoft. Cell surface area was calculated in microns and segmented based on a surface range (μm^2) as indicated.

Immunoblot Analysis

Protein samples were resolved by SDS-PAGE electrophoresis and then transferred to a PVDF membrane. The membrane-blocking procedure was carried out at room temperature in phosphate saline buffer (PBS) with 3% bovine serum albumin (BSA) and 0.3% tween solution. The primary antibody was incubated in a cold room overnight in PBS with 0.3% tween and 3% BSA; the membranes were then washed three times with a PBS 0.3% tween solution and incubated with a horseradish peroxidase-conjugated secondary antibody (GE Healthcare) in PBS 0.3% tween 3% BSA for one hour at room temperature. After three washes in a PBS 0.3% tween solution and incubation with the detection reagent (Millipore), the signal acquisition was performed using the Biorad ChemiDoc apparatus.

Analysis of plasma-branched chain amino acids and branched chain keto acids

25 µl plasma and standard was precipitated with 250 µl methanol containing one µM of deuterated internal standards (Valine-$^{13}C_5$,^{15}N, Leucine d_3, Isoleucine d_{10}, keto-leucine d_7, and keto-isoleucine d_8). After 10 minutes of vortexing at 1400 rpm, the samples were centrifuged at 4000 g for 10 minutes. 25 µl per sample were removed and evaporated under a stream of nitrogen gas. The samples were reconstituted in 125 µl water and injected into the UPLC-MS/MS system. Separation was performed on a Waters Acquity BEH C8 column (2.1 x 100mm 1.7µm) with a gradient consisting of water and acetonitrile, both with 0.1% formic acid. The detection was made on a Waters Xevo TQ-XS triple quadrupole mass

spectrometer in MRM mode using intra-run polarity switching where the detection of amino acids was made in positive mode between 0-3 minutes. The polarity was then switched to the negative mode for the detection of the keto acids between 3-10 minutes. The standard curve containing all six amino- and keto acids was prepared in 20% methanol and treated the same way as the samples.

Analysis of plasma acylcarnitines and glutamine

25µl of plasma was precipitated with 250 µl of methanol containing 1µM of deuterated glutamine. After 10 minutes of vortexing at 1400 rpm, the samples were centrifuged at 4000g for 10 minutes. 25µl µl was removed and evaporated under a stream of nitrogen gas. The samples were reconstituted in 125 µl of an acylcarnitine internal standard mix (NSK-B reference mix, Cambridge Isotope Laboratories) prepared in acetonitril:methanol [3:1]. The samples were separated in HILIC mode on a Waters BEH Amide column (2.1 x 100 1.7µm) using 5mM ammonium formate and 0.06% formic acid in 95% acetonitrile as mobile phase A and ten mM ammonium formate and 0.12% formic acid in 100% Milli-Q water as mobile phase B. The detection was made on a Waters Xevo TQ triple quadrupole mass spectrometer in positive MRM mode. Quantification of acylcarnitines was made using a one-point calibration against the deuterated analogue. For the acylcarnitines without a deuterated analogue, the quantification was made against the deuterated acylcarnitine closest in retention time. Glutamine was quantified using an external standard curve.

Glucose-stimulated insulin secretion in cultured pancreatic islets (GSIS)

Primary mouse islet isolation was performed as previously described (Hugill A. et al. 2016 PMID: 27584553). After isolation and overnight incubation at 37°C with humidified 5% CO_2 air in RPMI supplemented with 1% P/S and 10% FBS, islets were transferred into a 24-well plate. Five islets were hand-picked and transferred into each well in the presence of 200 µl low glucose buffer (Krebs Ringer Buffer KRB supplemented with 0.2% BSA and 2.8 mM glucose) and pre-incubated for 1 hour at 37°C. Islets underwent successive incubations for 20 minutes at 37°C with 200 µL of fresh KRB 0.2% BSA containing low glucose (2.8 mM), followed by high glucose (16.7 mM). At the end of each incubation, islets were transferred into a new well, and the supernatant was collected to measure insulin concentrations. At the end of the stimulation protocol, cells were lysed in 70 µl acid ethanol (75% absolute ethanol, 23.5% water, 1.5% HCl) and stored at four °C overnight. Samples were dried with a SpeedVac and resuspended in 30 µl ultrapure water. DNA was quantified by Nanodrop (ThermoFisher, USA), and insulin was quantified using an ELISA kit (Crystal Chem) and normalized to DNA content.

QUANTIFICATION AND STATISTICAL ANALYSIS

Data are expressed as means, and error bars indicate standard errors. Statistical significance is defined as $P<0.05$.

The exact number of mice used for each specific experiment is indicated in the figure legends, and we used littermate experimental and control mice.

Concerning sample size, for the in vivo time course experiments after the injection of PI3K inhibitors, we used a minimum of 5 mice. In an analysis where two different categorical variables are considered (e.g., GTT, ITT, mice weight gain, and time-course analyses), repeated measures (RM) two-way ANOVA was used unless indicated otherwise in the legend.

For all other in vivo studies, a minimum of 3 biological replicates were analyzed when parametric statistical tests were used, whereas a minimum of 4 biological replicates were analyzed when non-parametric statistical tests were used. For immunoblots, the parametric statistical test (t-test) was used to compare samples with three replicates on the same gel. For all other immunoblot analyses, we used a non-parametric test (Mann-Whitney).

All statistical analysis was performed using GraphPad Prism software.